WM RECORD COPY

SANDIA REPORT SAND84—0747 • Unlimited Release • UC—70
Printed January 1985

WM DOCKET CONTROL CENTER

'85 FEB 14 A10:36

FEMTRAN—A Finite Element Computer Program for Simulating Radionuclide Transport Through Porous Media

M. J. Martinez

Prepared by
Sandia National Laboratories
Albuquerque, New Mexico 87185 and Livermore, California 94550
for the United States Department of Energy
under Contract DE-AC04-76DP00789

HYDROLOGY DOCUMENT NUMBER 137

SF2900Q(3-81)

Issued by Sandia National Laboratories, operated for the United States Department of Energy by Sandia Corporation.
NOTICE: This report was prepared as an account of work sponsored by an agency of the United States Government. Neither the United States Government nor any agency thereof, nor any of their employees, nor any of their contractors, subcontractors, or their employees, makes any warranty, express or implied, or assumes any legal liability or responsibility for the accuracy, completeness, or usefulness of any information, apparatus, product, or process disclosed, or represents that its use would not infringe privately owned rights. Reference herein to any specific commercial product, process, or service by trade name, trademark, manufacturer, or otherwise, does not necessarily constitute or imply its endorsement, recommendation, or favoring by the United States Government, any agency thereof or any of their contractors or subcontractors. The views and opinions expressed herein do not necessarily state or reflect those of the United States Government, any agency thereof or any of their contractors or subcontractors.

Printed in the United States of America
Available from
National Technical Information Service
U.S. Department of Commerce
5285 Port Royal Road
Springfield, VA 22161

NTIS price codes
Printed copy: A05
Microfiche copy: A01

SAND84-0747
Unlimited Release
Printed January 1985

Distribution
Category UC-70

FEMTRAN - A Finite Element Computer Program for Simulating Radionuclide Transport Through Porous Media

M. J. Martinez
Fluid Mechanics and Heat Transfer Division
Sandia National Laboratories
Albuquerque, New Mexico 87185

ABSTRACT

FEMTRAN is a finite element computer program for numerical simulation of the two-dimensional transport of radionuclide decay chains through saturated/unsaturated sorbing porous media. Transport mechanisms include advection, hydrodynamic dispersion, diffusion, equilibrium adsorption, and radioactive decay and evolution. The mathematical formulation and numerical implementation are presented in some detail. User instructions and example problems are described to illustrate the use and capabilities of the program.

ACKNOWLEDGMENT

The present work is based upon the code developed by Duguid and Reeves and later upgraded by Yeh and Ward at Oak Ridge National Laboratory. The lucid coding and documentation of the parent codes proved to be of considerable advantage. The author is also grateful to N. E. Bixler for many useful discussions during this project.

PREFACE

FEMTRAN is a general purpose two-dimensional finite element computer program designed for simulation of radionuclide transport through porous media. The code was developed in support of the Nevada Nuclear Waste Storage Investigations* project to provide predictive capabilities for performance assessment and design specification. This report is intended to provide documentation of the FEMTRAN computer code. A complete description is given of the mathematical model and numerical solution procedure. Execution instructions are also provided for the users of the code.

Chapter I presents the equations governing radionuclide transport through saturated/unsaturated porous media along with the appropriate initial and boundary conditions. The remainder of the chapter is devoted to describing the solution of the transport equations by applying the method of weighted residuals technique to derive finite element equations. Chapter II lists the codes that are recognized by FEMTRAN for providing mesh and hydrodynamic data when required. These variables may also be provided by the user where appropriate. Chapter III provides complete user instruction for the execution of FEMTRAN. Job control language is also provided for execution on the SNLA CRAY-1S computer system. A set of sample problems are provided in Chapter IV to illustrate the use and capabilities of FEMTRAN. Computer output from Sample Problem 1 is provided in the appendix for check-out purposes.

Readers interested primarily in the use of FEMTRAN are urged to spend some time in the Governing Equations section of Chapter II. Understanding of the governing equations and initial and boundary condition requirements are essential to the successful application of FEMTRAN. User input requirements for execution are described in Chapters III and IV.

*The Nevada Nuclear Waste Storage Investigations Project, managed by the Nevada Operations Office of the U. S. Department of Energy, is examining the feasibility of siting a repository for high-level nuclear wastes at Yucca Mountain on and adjacent to the Nevada Test Site. This work was funded in part by the NNWSI Project. The ultimate use of this information will be for system analysis and performance assessment of a nuclear waste repository in tuff.

CONTENTS

		Page
	PREFACE	3
	FIGURES	5
	TABLES	6
	NOTATION	7
I.	INTRODUCTION	9
	Motivation	9
	Limitations and Assumptions	10
II.	MATHEMATICAL DESCRIPTION	11
	Governing Equations	11
	Finite Element Approximations	14
	Time Integration by Finite Differences	16
	Element Construction and Implementation	17
	Element Assembly	21
	Application of Boundary Conditions and Matrix Solution	21
	Mass Balance Computation	22
	Computation of Fluid and Radionuclide Flux	23
	Alternative Numerical Schemes	25
III.	COMPUTER INPUT REQUIREMENTS	26
	Mesh Specification	26
	Hydrodynamic Variables	26
IV.	USER INPUT INSTRUCTIONS	27
	Input Data Format	27
	User Supplied Subroutine	41
	Job Control Cards	42
V.	SAMPLE PROBLEMS	45
	One-Dimensional Transport -- Cauchy Boundary Condition	45
	One-Dimensional Transport -- Dirichlet Boundary Condition	50
	Two-Dimensional Transport -- Dirichlet Boundary Condition	56
	REFERENCES	68

FIGURES

Figure		Page
1	Global and Local Coordinate Systems	18
2	Orientation of Upstream Weighting Functions Along the Boundaries of a Transformed Element	20
3	Job Control Stream -- Run With User Subroutine	43
4	Job Control Stream -- Run With Disk Files	44
5	Input Data Deck for Sample Problem 1	46
6	Comparison Between Numerical (FEMTRAN) and Analytical (reference [20]) Solutions of Relative Concentration Profiles at 273 Years	48
7	Cumulative Mass Balance History for Sample Problem 1	49
8	Input Data Deck for Sample Problem 2	52
9	Activity History at 500 m From Source for Sample Problem 2	54
10	Cumulative Mass Balance History for Sample Problem 2	55
11	Finite Element Mesh Used for Sample Problem 3 (generated with QMESH [16])	57
12	Input Data Deck for Sample Problem 3	58
13	Activity History at x = 500 m, z = 0 for Sample Problem 3	59-61
14	Activity Profiles Along x = 500 m for Sample Problem 3. The time for each profile is at maximum breakthrough activity (see Table 3).	62
15	Contours of Activity for ^{234}U -- Sample Problem 3	63
16	Contours of Activity for ^{230}Th -- Sample Problem 3	65
17	Contours of Activity for ^{226}Ra -- Sample Problem 3	66
18	Cumulative Mass Balance History for Sample Problem 3	67

TABLES

		Page
1.	Optional Finite Element Schemes	25
2.	Radionuclide Properties	45
3.	Transport Parameters	47
4.	Long-Lived Parent Nuclide	50
5.	Retention Factors	51
6.	Maximum Activity	56

NOTATION

a_L	Longitudinal dispersivity (L)
a_T	Transverse dispersivity (L)
A_{IJ}	Elemental coefficient matrix
B_1	Domain boundary with Dirichlet conditions
B_2	Domain boundary with Neumann conditions
B_3	Domain boundary with Cauchy conditions
C	Volumetric mass concentration (M/L^3)
$\dot{C}$	Time derivative of the concentration (M/L^3T)
D_d	Molecular diffusion coefficient (L^2/T)
D_{ij}	Dispersion-diffusion tensor (L^2/T)
D_I	Elemental load vector due to sources
E_{IJ}	Elemental boundary flux matrix for Cauchy boundaries
F_I	Elemental force vector
h	Fluid pressure head (L)
$[J]$	Jacobian matrix
J	Determinant of [J]
k_{ij}	Hydraulic conductivity tensor (L/T)
K_d	Distribution coefficient (L^3/M)
$L(\cdot)$	Differential operator
M_{IJ}	Elemental mass (capacitance) matrix
n_i	Outward pointing unit normal vector
N_I	Basis functions
q	Nuclide source
q_3	Cauchy boundary flux (M/L^2T)
Q_I	Elemental load vector due to boundary fluxes
R	Computational region

R_d	Retention factor
R^e	Region of element e
R_{res}	Elemental residual error
S	Solid phase concentration of adsorbed species (M/M)
S_{IJ}	Elemental stiffness matrix
t	Time (T)
T_{IJ}	Global coefficient matrix
U_i	Darcy velocity vector (L/T)
W_I	Weighting functions
$x_i(x,z)$	Spatial coordinates (L)
Y_I	Global force vector

Greek Symbols

α'	Modified coefficient of compressibility of medium
δ_{ij}	Kronecker delta
θ	Moisture content (L^3/L^3)
λ	Radioactive decay coefficient (1/T)
ξ,η	Local coordinates
ρ	Bulk density of medium (M/L^3)
τ	Tortuosity
ω	Timeplane weighting factor

Superscript

m	Refers to the m-th member of an M-membered decay chain

Subscripts

i,j	Standard indicial notation in tensor analysis
I,J	Refers to quantities resulting from application of the finite element method

I. INTRODUCTION

Motivation

A major task of the Nevada Nuclear Waste Storage Investigations (NNWSI) project is to provide performance assessment and evaluation of a candidate repository site in the Yucca Mountain region of the Nevada Test Site. Nuclear waste composition includes many long-lived radionuclides that produce daughter nuclides by first-order reaction. The need for predicting radionuclide transport by groundwater from repository to biosphere has prompted the development of the FEMTRAN computer code described in this report. FEMTRAN simulates the transport of a chain of radionuclides through a two-dimensional saturated or unsaturated porous medium. Radionuclide decay chain reactions considered here may be described as,

$$C^1 \rightarrow C^2 \rightarrow C^3 \rightarrow \ldots \rightarrow C^m$$

where C^m denotes liquid phase volumetric mass concentration of the m-th nuclide in the chain and the evolution of each daughter species $(C^m,\ m > 1)$ is by first order decay of its precursor. The transport mechanisms for each nuclide include the effects of advection, hydrodynamic dispersion, diffusion, equilibrium adsorption and first order decay and evolution. The resulting equations are solved by applying the method of weighted residuals in the context of the finite element method. The resulting ordinary differential equations are integrated in time by standard finite difference recurrence relations (Crank-Nicolson, backward difference, mid-difference). Matrix equations are solved by Gaussian elimination.

The basis of the code FEMTRAN is the transport code developed by Duguid and Reeves[1] and subsequently modified and expanded by Yeh and Ward[2] at Oak Ridge National Laboratory. The code FEMWASTE (Yeh and Ward[2]) was designed to model transport of one species of the type described here without evolution from a precursor and under steady boundary conditions. In addition to handling chain decay and transient boundary conditions, the transport equation has been rearranged into a more suitable form for computing with numerically generated space and time dependent hydrodynamic solutions. The rearranged equations require a modified numerical implementation of the Cauchy (third-type) boundary condition. With the addition of decay chains, certain parameters now vary with material type as well as species. The

parameters include species decay, equilibrium adsorption, and molecular diffusion coefficients. The remaining parameters are assumed to depend only on the medium through which the radionuclides are being transported. Various additional modifications to the parent code are explained in the subsequent text.

The many similarities between FEMTRAN and FEMWASTE will become evident in the structure of this report. The input format and symbolic notation will also be familiar to previous users of FEMWASTE. Although a conscious effort was made to provide completeness in this document, users of FEMTRAN may find documentation of the parent codes[1,2] valuable.

Limitations and Assumptions

Although FEMTRAN was designed as a general purpose radionuclide transport model, the various limitations and assumptions are listed for the convenience of the user. The following should aid in deciding the applicability of FEMTRAN to the problem at hand.

(1) The problem geometry is limited to the plane.

(2) Decay chain reactions are assumed to be of the first-order type. Only sequential decay chains are considered. The program is dimensioned for up to ten-membered decay chains.

(3) Ten different homogeneous material types may be included.

(4) Hydrodynamic dispersion is described as a Fickian process for a homogeneously dispersing medium.

(5) Adsorption reactions with the medium are described by an equilibrium isotherm.

II. MATHEMATICAL DESCRIPTION

This section presents the mathematical formulation describing the advective-dispersive transport of a chain of radionuclides through a saturated/unsaturated sorbing porous medium. The numerical solution method and implementation are also discussed in some detail.

Governing Equations

The equations describing the transport of a chain of radionuclides through a sorbing porous medium are a statement of mass balance. The transport equations presented here include the mechanisms of advection, hydrodynamic dispersion, molecular diffusion, linear equilibrium adsorption and first-order radioactive decay and evolution. The transport equation for the m-th radionuclide may be written (c.f. Yeh and Ward[2] and Bear[3]), for transport in the plane, as

$$
\begin{aligned}
L(C^m) = {} & \frac{\partial}{\partial t}\left(\theta C^m + \rho S^m\right) + \left(\theta C^m + \rho S^m\right)\alpha' \frac{\partial h}{\partial t} \\
& + \frac{\partial}{\partial x_i}\left(U_i C^m - \theta D^m_{ij} \frac{\partial}{\partial x_j} C^m\right) \qquad (1) \\
& + \lambda^m\left(\theta C^m + \rho S^m\right) - \lambda^{m-1}\left(\theta C^{m-1} + \rho S^{m-1}\right) - q^m = 0 \quad ,
\end{aligned}
$$

$$
\begin{aligned}
i &= x,z \\
m &= 1,\ldots,M
\end{aligned}
$$

Summation is implied by repeated indices. Equation (1) becomes valid for $m = 1$ by formally setting λ^0 to zero. The first term represents the rate of storage of total mass (including dissolved and adsorbed phases) in the considered region. The second term includes the change in storage by compaction of the bulk volume due to pressure. The third term is the divergence of material flux by advection, dispersion, and diffusion. The fourth and fifth terms represent the first-order decay and evolution of the m-th nuclide, respectively. The last term is the input of material by the nuclide source. The dispersion-diffusion tensor, assuming an isotropic (for dispersion) medium[3], is given by,

$$\theta D^m_{ij} = (a_T U + \theta D^m_d \tau)\delta_{ij} + (a_L - a_T)U_i U_j / U \tag{2}$$

where ,

$$U = \sqrt{U_i U_i} \quad , \quad i = x,z$$

is the magnitude of the Darcy velocity.

In deriving (1) the hydrodynamic variables, $\theta(x_i,t)$, $h(x_i,t)$, and $U_i(x_i,t)$ are assumed known inputs. When considering general time-dependent saturated/unsaturated transport problems, the fields are given by solving the hydrodynamic problem. The Darcy velocities, U_i, are obtained by applying the Darcy equation to the hydraulic head solution.

The adsorption of radionuclides by the porous skeleton is assumed to occur on a time scale that is small compared to the transport time scale so that the dissolved and adsorbed phases are in equilibrium. For small solution concentrations the adsorbed concentration is given by the linear equation,

$$S^m = K^m_d C^m \tag{3}$$

where K^m_d is the equilibrium distribution coefficient for the m-th nuclide. Substitution of (3) into (1) gives,

$$\begin{aligned} L(C^m) = {} & \theta R^m_d \frac{\partial}{\partial t} C^m + U_i \frac{\partial}{\partial x_i} C^m - \frac{\partial}{\partial x_i} \theta D^m_{ij} \frac{\partial C^m}{\partial x_j} \\ & + \theta R^m_d C^m \alpha' \frac{\partial h}{\partial t} + \lambda^m \theta R^m_d C^m - \lambda^{m-1} \theta R^{m-1}_d C^{m-1} \\ & - q^m = 0 \end{aligned} \tag{4}$$

where,

$$R^m_d = 1 + \frac{\rho K^m_d}{\theta}$$

is the retention factor. The fluid mass balance equation,

$$\frac{\partial \theta}{\partial t} = -\frac{\partial}{\partial x_i} U_i$$

has been used in arriving at (4).

The initial conditions for (4) are given by,

$$C^m = C_i^m (x_i, t) \quad \text{at} \quad t = 0 \text{ in } R \quad , \quad m = 1, \ldots, M \tag{5}$$

where C_i^m are given functions of x_i. The boundary conditions for (4) may be Dirichlet, expressed as,

$$C^m = C_1^m (x_i, t) \quad \text{on} \quad B_1 \quad , \quad m = 1, \ldots, M \tag{6}$$

Neuman, expressed as,

$$\theta D_{ij}^m \frac{\partial C^m}{\partial x_j} n_i = 0 \quad \text{on} \quad B_2 \quad , \quad m = 1, \ldots, M \tag{7}$$

or Cauchy expressed as,

$$(U_i C^m - \theta D_{ij}^m \frac{\partial C}{\partial x_j}) n_i = q_3^m (x_i, t) \quad \text{on} \quad B_3 \quad , \quad m = 1, \ldots, M \tag{8}$$

where $B = B_1 \cup B_2 \cup B_3$ is the total system boundary. When simulating geologic nuclear waste repositories, the appropriate forms of C_1^m and q_3^m are given by the Bateman equations[4,5]. Bateman's equations are the solutions to the mass balance equations,

$$\frac{dC_1^m}{dt} = -\lambda^m C_1^m + \lambda^{m-1} C_1^{m-1} \quad , \quad m = 1, \ldots, M \tag{9}$$

$$(\lambda^\circ = 0)$$

which must be satisfied at the repository due to mass evolution and decay. The solutions[4,5] to (9) are given by,

$$C_1^j(t) = \sum_{p=1}^{m} \frac{C_o^p}{\lambda_m} \prod_{r=p}^{m} \lambda_r \sum_{q=p}^{m} \frac{e^{-\lambda_q t}}{\prod_{\substack{s=p \\ s\neq p}}^{m} (\lambda_s - \lambda_q)} \tag{10}$$

where C_o^m is the initial repository inventory for the m-th nuclide. The Dirichlet condition is given directly by (10). The Cauchy condition is given by the vector product,

$$q_3^m = C_1^m U_i n_i \quad \text{on} \quad B_3 \quad .$$

Finite Element Approximations

Approximate solutions to the transport equations (4) subject to appropriate initial and boundary conditions (5), (6), (7), (8) are obtained by applying the method of weighted residuals (MWR). A detailed description of the method has been given by Heubner and Thornton[6], among others. Additional descriptions can be found in reports by Yeh and Ward[2] and Duguid and Reeves.[1]

To apply the MWR, the computational domain is subdivided into an assemblage of smaller sub-domains referred to as finite elements. The dependent variable, C^m, is approximated by $\hat{C}^m$ in each element with,

$$C^m \cong \hat{C}^m = \sum_{I=1}^{4} C_I^m(t) N_I(x_i) \tag{11}$$

where N_I are the trial (basis) functions approximating the spatial variation of C^m in the element, and $C_I^m(t)$ are the unknown time-dependent nodal values of concentration for the m-th nuclide. Bilinear basis functions defined on quadrilaterals are used for the N_I. Substitution of (11) into the governing equations results in a set of equations with some residual error, R_{res}. The MWR chooses the unknown functions C_I^m such that the residual vanishes over the element domain in some weighted average sense. The weighted residual is set to zero by requiring

$$\int_{R^e} W_I L(\hat{C}^m) dR = \int_{R^e} W_I R_{res} dR = 0 \quad , \quad I = 1,\ldots,4 \tag{12}$$

where W_I are the weighting functions used to form the weighted average. Application of (12) results in the following matrix equation for element e,

$$[M^m_{IJ}]\{\dot{C}^m_J\} + [S^m_{IJ}]\{C^m_J\} + \{D^m_I\} + \{Q^m_I\} = 0 \tag{13}$$

where,

$$\dot{C}^m_I = \frac{d}{dt} C^m_I \tag{14a}$$

$$M^m_{IJ} = \int_{R^e} \theta R^m_d W_I N_J dR \tag{14b}$$

$$S^m_{IJ} = \int_{R^e} U_i W_I \frac{\partial N_J}{\partial x_i} + \theta D^m_{ij} \frac{\partial W_I}{\partial x_j} \frac{\partial N_J}{\partial x_i} + \theta R^m_d \left(\alpha' \frac{\partial h}{\partial t} + \lambda^m\right) W_I N_J \quad dR \tag{14c}$$

$$D^m_I = - \int_{R^e} W_I \left(\theta R^{m-1}_d \lambda^{m-1} C^{m-1} + q^m\right) dR \tag{14d}$$

$$Q^m_I = - \int_{B^e} \theta D^m_{ij} W_I \frac{\partial C^m}{\partial x_j} n_i \; dB \tag{14e}$$

The divergence term in (4) has been integrated by parts (Greens Theorem) in arriving at Equation (14).

Yeh and Ward[2] found that mass matrix lumping is often desirable when using central or backward-difference time marching and provide this option in their report. The lumping is performed by performing a row sum on M_{IJ} as follows,

$$M^m_{II} = \sum_{J=1}^{4} \int_{R^e} \theta R^m_d \; W_I N_J \; dR \tag{15}$$

and,

$$M^m_{IJ} = 0 \quad , \quad I \neq J$$

where no summation is taken over I in (15). This option is retained in FEMTRAN.

Time Integration by Finite Differences

Application of the MWR to the governing equations results in a set of simultaneous ordinary differential equations in time given by (13). The integration in time of (13) by finite difference results in an element matrix equation given by,

$$[A^m_{IJ}]\{C^m_J\} = \{F^m_I\} \tag{16}$$

when the $[A^m_{IJ}]$ and $\{F^m_I\}$ depend on the timeplane weighting parameter ω specifying an intermediate time $t_\omega = t + \omega\Delta t$ between a time step Δt.

In general, the coefficient matrix and forcing vector are given by,

$$[A^m_{IJ}] = [M^m_{IJ}]/\Delta t + \omega[S^m_{IJ}]$$

$$\{C^m_J\} = \{C^m_J\}_{t+\Delta t}$$

$$\begin{aligned}\{F^m_I\} = &([M^m_{IJ}]/\Delta t - (1-\omega)[S^m_{IJ}])\{C^m_J\}_t \\ &-(1-\omega)(\{D^m_I\}_t + \{Q^m_I\}_t) \\ &-\omega(\{D^m_I\}_{t+\Delta t} + \{Q^m_I\}_{t+\Delta t})\end{aligned} \tag{17}$$

where $[M^m_{IJ}]$ and $[S^m_{IJ}]$ are evaluated at t_ω. The Crank-Nicolson centered-in-time formulation is given by $\omega = 1/2$ and the backward-difference formulation by $\omega = 1$. The mid-difference method[2] assumes a linear variation of variables in time over the time step Δt such that,

$$\{\dot{C}_J^m\} = \left(\{C_J^m\}_{t+\Delta t/2} - \{C_J\}_t\right)/(\Delta t/2)$$

$$\{C_J^m\}_{t+\Delta t} = 2\{C_J^m\}_{t+\Delta t/2} - \{C_J^m\}_t \tag{18}$$

which results in,

$$[A_{IJ}^m] = 2[M_{IJ}^m]/\Delta t + [S_{IJ}^m]$$

$$\{C_J^m\} = \{C_J^m\}_{t+\Delta t/2}$$

$$\{F_I^m\} = (2[M_{IJ}^m]/\Delta t)\{C_J^m\}_t \tag{19}$$

$$- \{D_I^m\}_{t+\Delta t/2} - \{Q_I^m\}_{t+\Delta t/2}$$

for the element matrix (16). Equation (18) gives the values of $\{C_J^m\}_{t+\Delta t}$.

Element Construction and Implementation

The four node, bilinear quadrilateral element was used for approximating the spatial distribution of variables. In terms of the local coordinate system given in Figure 1, the bilinear basis function[6,7] is written as,

$$N_I(\xi,\eta) = \frac{1}{4}(1 + \xi\xi_I)(1 + \eta\eta_I) \qquad I = 1,\ldots,4 \tag{20}$$

where ξ_I and η_I are the local coordinates of the corner nodes numbered from 1 to 4 in a clockwise direction around the element. In Galerkin's formulation of the method of weighted residuals, the weighting functions, W_I, are set equal to the basis functions N_I. For advection dominated problems, researches have found it advantageous to use weighting functions that give a greater weighting to the upstream nodes connected to the considered node[8-10]. The upstream formulation of the method of weighted residuals uses weighting functions[10] given by,

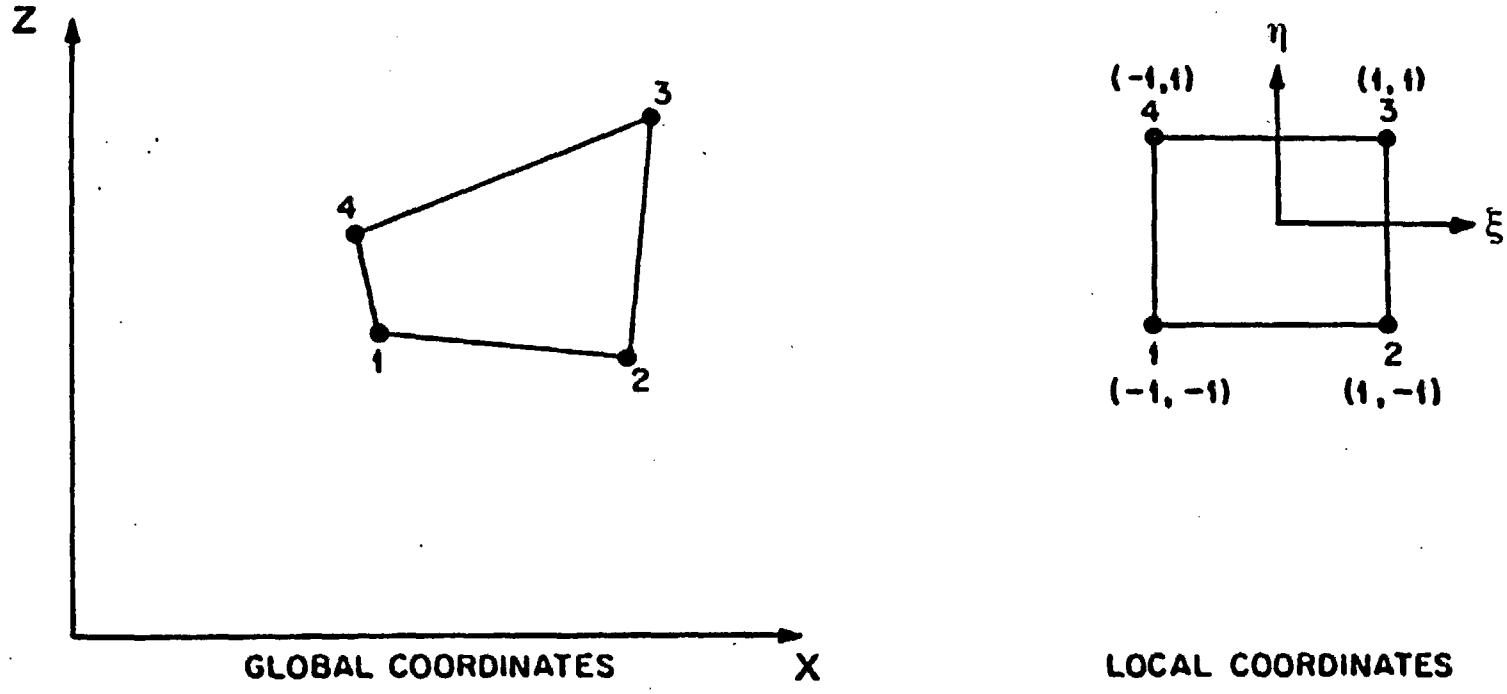

Figure 1. Global and Local Coordinate Systems (from Ref. 1)

$$W_1 = \frac{1}{16}\left[(1+\xi)(3\alpha_1\xi - 3\alpha_1 - 2) + 4\right]\left[(1+\eta)(3\beta_2\eta - 3\beta_2 - 2) + 4\right]$$

$$W_2 = \frac{1}{16}\left[(1+\xi)(-3\alpha_1\xi + 3\alpha_1 + 2)\right]\left[(1+\eta)(3\beta_1\eta - 3\beta_1 - 2) + 4\right]$$

$$W_3 = \frac{1}{16}\left[(1+\xi)(-3\alpha_2\xi + 3\alpha_2 + 2)\right]\left[(1+\eta)(-3\beta_1\eta + 3\beta_1 + 2)\right]$$

$$W_4 = \frac{1}{16}\left[(1+\xi)(3\alpha_2\xi - 3\alpha_2 - 2) + 4\right]\left[(1+\eta)(-3\beta_1\eta + 3\beta_2 + 2)\right]$$

where α_1, α_2, β_1, β_2 are upstream weighting factors associated with sides 1-2, 2-3, 4-3, and 1-4, respectively, of an element as illustrated in Figure 2. The weighting parameters[8] are given by,

$$\alpha(\text{or } \beta) = \coth\left(\frac{UL}{2D}\right) - \frac{2D}{UL} \tag{21}$$

where the U, L, D represent the velocity component, length and dispersion coefficient along the corresponding element side (Figure 2). Equation (21) was derived by equating the analytical and numerical solution with upstream weighting of steady, one-dimensional convective-diffusive transport[8].

The transformation between global and local coordinates is given by,

$$x_i = x_{iJ}N_J(\xi,\eta) \tag{22}$$

where the x_{iJ} are the global node coordinates and N_J are interpolation functions for the element. An isoparametric mapping is selected where the N_J are the same as the basis functions.

The construction of the element equations given in (14) requires evaluation of various derivatives and integrals of the basis functions. The transformation of derivatives between local and global planes is given by,

$$\begin{matrix} \frac{\partial}{\partial\xi} \\ \frac{\partial}{\partial\eta} \end{matrix} = \begin{bmatrix} \frac{\partial x}{\partial\xi} & \frac{\partial z}{\partial\xi} \\ \frac{\partial x}{\partial\eta} & \frac{\partial z}{\partial\eta} \end{bmatrix} \begin{matrix} \frac{\partial}{\partial x} \\ \frac{\partial}{\partial z} \end{matrix} = [J] \begin{matrix} \frac{\partial}{\partial x} \\ \frac{\partial}{\partial z} \end{matrix} \tag{23}$$

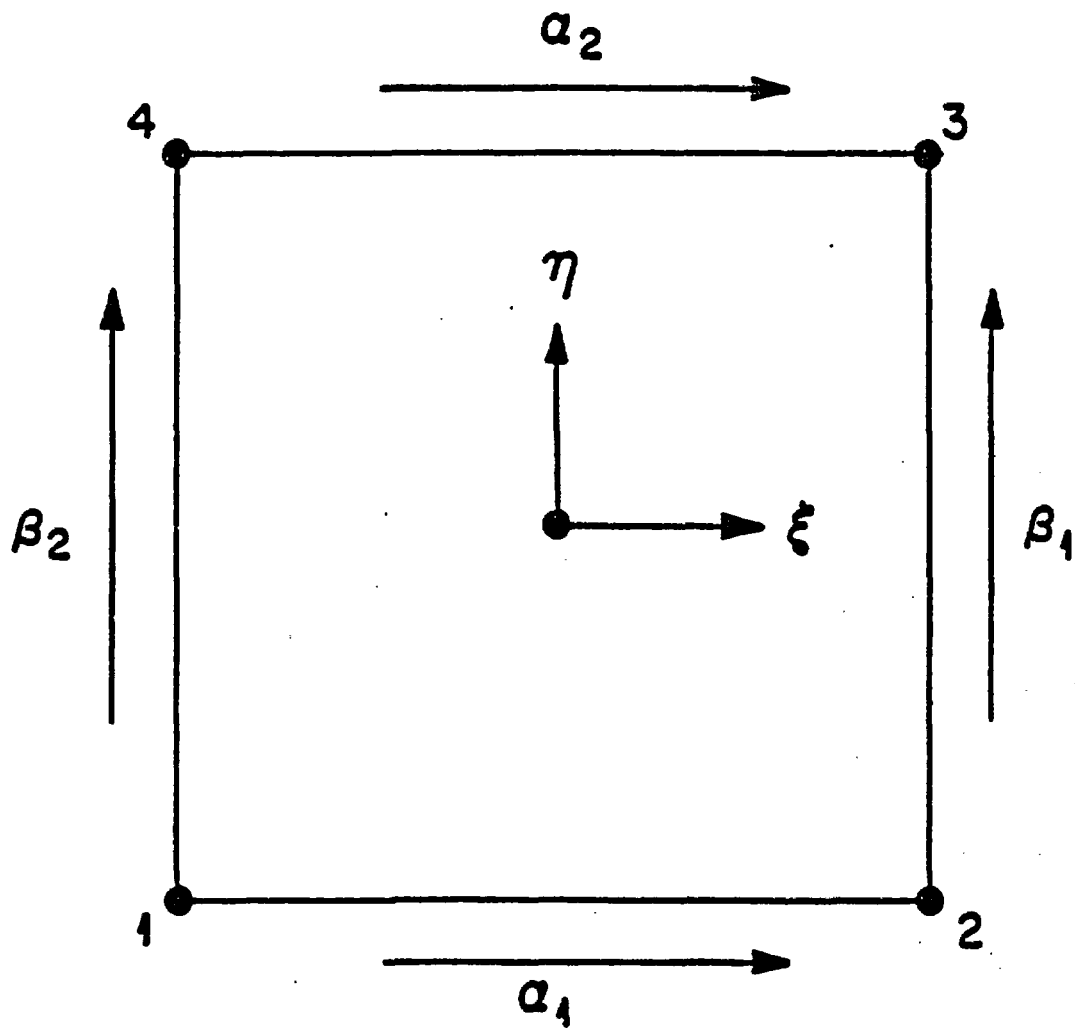

Figure 2. Orientation of Upstream Weighting Functions Along the Boundaries of a Transformed Element (from Ref. 2)

where [J] is the Jacobian matrix. Inversion of (23) gives the required relationship for use in (14). The final transformation required for numerical computation of (14) is the elemental area in local coordinates. In the plane, this is given by,

$$dxdz = J\, d\xi d\eta \tag{24}$$

where J is the determinant of [J]. The numerical integration of the transformed versions of (14) is performed using 2 X 2 Gaussian quadrature.

Element Assembly

Equations presented thus far have represented the region of a single finite element. The entire computational region is represented by generating an equation of the form (16) for all elements by assembling the equations such that inter-element continuity is enforced. This is accomplished by appropriate summation of equations such that unknowns at nodes common to adjacent elements are the same in all elements connecting at that node, i.e., the "direct stiffness method."[6] The resulting matrix is of the form,

$$[T_{IJ}]\{C_J^m\} = \{Y_I\} \tag{25}$$

The global coefficient matrix $[T_{IJ}]$ is banded and sparse. To reduce storage requirements only the banded portion is stored[1,11].

Application of Boundary Conditions and Matrix Solution

Dirichlet boundary conditions are applied by modifying $[T_{IJ}]$ and $\{Y_I\}$ in (25) such that the equations for the prescribed C_J^m are identically satisfied. The procedure is outlined in References 1 and 6.

The Neumann condition (7) is applied by setting Q_I^m in (14c) to zero. This is the natural boundary condition for (4) and as such is the default boundary condition when no other is specified.

The Cauchy condition is applied by substituting (8) into (14c). This boundary condition is implemented by specifying,

$$\{Q_I^m\} = \int_{B^e} W_I\ \{q_3^m\} dB \tag{26}$$

and adding to $[S^m_{IJ}]$,

$$[E^m_{IJ}] = -\int_{B^e} W_I U_i n_i N_J \, dB \tag{27}$$

The vector and matrix, (26) and (27), are incorporated into the elemental equations by the procedure outlined in (17), (18), or (19), depending on the time integration scheme, and assembled into (25).

The matrix equation (25), having been modified for boundary conditions, is solved by Gaussian elimination.

Mass Balance Computation

A mass balance check on a computed solution can be obtained by considering the integral form of the governing equations over the entire computational region. A mass balance check serves as an indicator of the accuracy and consistency of the computer code. Mass balance computations are provided for the nuclide concentration distributions and fluid flow fields since the former is a result of the latter (except in diffusion dominated problems). The fluid mass balance is an indication of the accuracy of the input flow field used to compute nuclide transport.

The fluid mass balance can be checked by comparing the boundary flux with the accumulation of mass within the computational region. The mass divergence rate is given by,

$$\int_B U_i n_i \, dB \tag{28a}$$

and the accumulation rate by,

$$\int_R \left(\frac{\partial \theta}{\partial t}\right) dR \tag{28b}$$

These are components of the mass balance equation written in integral form for the entire computational region. The boundary flux term (28a) is broken into three terms, one for each type of boundary (Dirichlet, Neumann and Cauchy) that constitute the entire mesh boundary, B. Ideal mass balance would be indicated if the accumulation and divergence functions sum to zero. However, in any numerical simulation these terms can only be expected to sum to some acceptably small value.

In a similar manner, an indication of the accuracy and consistency of the solution computed for each nuclide is given by mass balance. Radionuclide mass divergence rate for the m-th species is given by,

$$\int_B \left(U_i C^m - \theta D^m_{ij} \frac{\partial C^m}{\partial x_j}\right) n_i \, dB \tag{29a}$$

and the net accumulation rate by,

$$\int_R \left(\frac{\partial}{\partial t} \theta C^m + \frac{\partial}{\partial t} \rho S^m + \lambda^m \theta R^m_d C^m - \lambda^{m-1} \theta R^{m-1}_d C^{m-1} + \alpha' \theta R^m_d \frac{\partial h}{\partial t} C^m - q^m\right) dR \tag{29b}$$

As in the fluid balance procedure, the divergence function is broken into three terms for clear identification of the boundary flux contribution from each boundary type.

Computation of Fluid and Radionuclide Flux

In formulating the governing equations for radionuclide transport, the Darcy velocity field was assumed to be a known input. The hydrologic solution is obtained from a hydrodynamic code when simulating time-dependent saturated/unsaturated problems. The usual dependent variable in hydrodynamic codes is hydraulic head. Darcy velocities are obtained from the hydraulic head field by application of the Darcy equation. FEMTRAN offers the option of computing Darcy velocities from the hydrodynamic solution by application of Galerken's method of weighted residuals to the Darcy equation. This is expressed as,

$$\int_{R^e} N_I \left(U_{iJ} N_J + k_{ij} \frac{\partial N_J}{\partial x_j} h_J\right) dR^e \quad , \quad \begin{array}{l} I = 1,\ldots,4 \\ i = x,z \end{array} \tag{30}$$

where U_{iJ} are the nodal values of the i component of Darcy velocity. The application of Galerkin's method results in the following elemental matrix equation,

$$[G_{IJ}]\{U_{iJ}\} = \{H_{iI}\} \quad , \quad i = x,z \tag{31}$$

where,

$$[G_{IJ}] = \int_{R^e} N_I N_J \, dR$$

$$\{H_{iI}\} = - \int_{R^e} k_{ij} N_I \frac{\partial N_J}{\partial x_j} h_J \, dR$$

The equations are assembled for all elements and solved by Gaussian elimination. This option was incorporated for use with the hydrodynamic codes[12,13] developed in the Fluid and Thermal Sciences Department at SNLA which have the option of computing Darcy velocity according to,

$$U_i^s = -k_{ij} \frac{\partial N_I}{\partial x_j} h_I \tag{32}$$

applied on an element basis. In fact, the present option for computing Darcy velocities uses those values directly in the force vector, i.e.,

$$\{H_{iI}\} = \int_{R^e} N_I U_{iJ}^s N_J \, dR \tag{33}$$

where U_{iJ}^s are nodal point values of Darcy velocity. This numerical implementation of computing Darcy velocities has proven superior in some circumstances[2,14].

The computation of radionuclide flux is performed in an analogous manner to the fluid flux. Equation (31) becomes,

$$[G_{IJ}]\{F_{iJ}^m\} = \{H_{iI}^m\} \tag{34}$$

where,

$$[G_{IJ}] = \int_{R^e} W_I N_J \, dR$$

$$\{H^m_{iI}\} = - \int_{R^e} W_I \left(\theta D^m_{ij} \frac{\partial N_J}{\partial x_j} - U_i N_J\right) C^m_J \, dR$$

The equations are assembled and solved as before for each radionuclide in the chain.

Alternative Numerical Schemes

All numerical schemes reported by Yeh and Ward[2] remain operational in this work. The 12 options are listed in Table 1 (from Reference 2).

Table 1. Optional Finite Element Schemes

Schemes	Time-marching methods			Weighting function		Mass matrix lumping	
	Crank-Nicolson	Backward-difference	Mid-difference	Galerkin	Upstream	No	Yes
1	x			x		x	
2		x		x		x	
3	x				x	x	
4	x			x			x
5	x				x		x
6		x			x	x	
7		x		x			x
8		x			x		x
9			x	x		x	
10			x		x	x	
11			x	x			x
12			x		x		x

III. COMPUTER INPUT REQUIREMENTS

The computer code FEMTRAN was designed for general purpose simulation of radionuclide transport. The following outlines the input requirements needed for simulating a general transport problem and the compatibilities with other codes.

Mesh Specification

Finite element meshes may be specified by the user or from disk file. The mesh generation subroutines in FEMWATER[15] have been included in FEMTRAN to allow user mesh specification. The finite element mesh data may also be read from disk unit 9 after construction with the mesh generator code QMESH[16] or from DECODE[17]. DECODE is a mesh and solution transfer code for using hydrodynamic mesh and solution data generated with SAGUARO[13] or MARIAH[12].

Hydrodynamic Variables

In writing the governing equations, (1) through (8), it was assumed that the hydrodynamic variables θ, U_i, and h, as functions of space and time, were known inputs. In general, these variables are computed by solving the hydrodynamic problem prior to performing the radionuclide simulation. The hydrodynamic solution may be computed for use in FEMTRAN with the following codes,

FEMWATER[15]

MARIAH[12] (using DECODE[17] or MERLIN[18] for data transfer)

SAGUARO[13] (using DECODE[17] or MERLIN[18] for data transfer)

A linear timeplane interpolation procedure is included in FEMTRAN so that the transport calculation need not proceed at the same time-stepping sequence used in computing the hydrodynamic solution. Different time scales for the two phenomena may be resolved in this manner. The hydrodynamic solution may also be specified through a user subroutine, allowing specification of a general space (two-dimensional) and time dependent solution (e.g., a source-sink well pair).

IV. USER INPUT INSTRUCTIONS

This chapter describes the sequence of inputs required for executing FEMTRAN. The data sets are listed in the order anticipated by FEMTRAN. The input structure is very similar to Reference 2 for the convenience of those familiar with the execution of FEMWASTE. Each data set in the input list is structured as follows.

1) Following the data set number, data set title, and format for the typed data, a brief description of the information contained on the card is given. Included in this information are the circumstances under which the card is required and how many cards of the same type will be read (e.g., when simulating decay chains).
2) The variable name used in the code, the columns and format in which the data is typed, and a description of the variable is given for each data entry.
3) The card number indicates how many cards will be expected for that data set.
4) Several jobs may be computed in one execution by cascading the sequence of data sets for each job. The user is reminded to check that disk data, if required, is provided correctly in the job control input stream.

Input Data Format

The following data sets are described in this section.

Data Set 1: Problem Identification
Data Set 2: Control Parameters
Data Set 3: Conversion Factors
Data Set 4: Dirichlet Boundary Control
Data Set 5: Cauchy Boundary Control
Data Set 6: Time Integration Parameters
Data Set 7: Printed Output Control
Data Set 8: Auxiliary Storage and Flow Field Control
Data Set 9: Material Properties
Data Set 10: Species and Material Dependent Properties
Data Set 11: Nodal Point Coordinates
Data Set 12: Element Connectivity
Data Set 13: Material Correction
Data Set 14: Initial Conditions
Data Set 15: Dirichlet Boundary Conditions
Data Set 16: Neumann Boundary Conditions
Data Set 17: Cauchy Boundary Conditions

Data Set 1 — Problem Identification — FORMAT (I5,9A8)

This data set provides a problem number and title for easy identification of job.

Card	Variable	Column	Format	Definition
1	NPROB	1-5	I5	Problem number
	TITLE	6-77	9A8	Problem title

Data Set 2 — Control Parameters — FORMAT (16I5)

The specification of control parameters for defining the problem are given in this data set.

Card	Variable	Column	Format	Definition
1	NNP	1-5	I5	Total number of nodal points in problem
	NEL	6-10	I5	Total number of elements in problem
	NMAT	11-15	I5	Number of materials
	NCM	16-20	I5	Number of elements with corrected material properties
	NTI	21-25	I5	Number of time increments
	NBCT	26-30	I5	Dirichlet boundary control; 0 = no Dirichlet boundaries in this problem, 1 = Dirichlet boundaries will be specified
	NSTT	31-35	I5	Cauchy boundary control; 0 = no Cauchy boundaries in this problem 1 = Cauchy boundaries will be specified
	KVI	36-40	I5	Flow field input control; 1 = steady-state flow field will be specified, 2 = transient flow field will be specified

	KSTR	41-45	I5	Auxiliary solution storage control; 0 = solution will not be stored, 1 = solution is stored on unit 2 (see Data Set 8 for specifying timeplanes to be stored)
	KSS	46-50	I5	Steady state control; 0 = steady state solution, 1 = transient solution
	NMPPM	51-55	I5	Number of material properties per material (see Data Set 9)
	WET	56-60	I5	Weighting function control; 0 = Galerkin formulation, 1 = upstream weighting
	ILUMP	61-65	I5	Mass matrix lumping control; 0 = mass matrix will not be lumped 1 = mass matrix is lumped
	IMID	66-70	I5	Mid-difference control; 0 = no mid-difference integration 1 = mid-difference time algorithm is specified
2	NSPEC	1-5	I5	Number of species in decay chain ($1 \leq NSPEC \leq 10$)
	ITRBC	6-10	I5	Transient Boundary Condition Control; 0 = steady-state boundary conditions, 1 = transient boundary conditions are specified (see Equation (10))
	IMESH	11-15	I5	Mesh input control; 0 = mesh data will be specified by user 1 = mesh data will be read from logical unit 9
	IHYDRO	16-20	I5	Hydrodynamic solution input control; 0 = hydrodynamic solution is computed in user subroutine,

			1 = solution read from logical unit 1 as generated with DECODE[17]*, or, 2 = solution generated with MERLIN [18]**, or, 3 = solution generated with FEMWATER***
ICONFLW	21-25	I5	Continuous velocity control; 0 = velocities will not be computed 1 = velocities will be computed by applying Galerkin's method
MASBAL	26-30	I5	Hydrodynamic mass balance control; 0 = hydrodynamic balance is not computed, 1 = balance is computed

---

Data Set 3 — Conversion Factors — FORMAT(8F10.0)

This data set is needed only when IHYDRO=1 or 2 (Data Set 2) which specifies that the hydrodynamic solution will be computed with SAGUARO.[13] SAGUARO computes effective pressure, $P = p + \rho gz$, as dependent variable in units of pressure. The parameters HCONV and VCONV may be used to convert between SAGUARO and FEMTRAN units.

Card	Variable	Column	Format	Definition
1	HCONV	1-10	F10.0	Head conversion factor
	VCONV	11-20	F10.0	Darcy velocity conversion factor

*data is read by,

```
    READ(1)TIME,(HT(NP),NP=1,NNP),(TH(M,IQ),IQ=1,4),M=1,NEL),
   >((VX(M,IQ),IQ=1,4),M=1,NEL),((VZ(M,IQ),IQ=1,4),M=1,NEL)
```

**data is read by,

```
    READ(1)TIME,(HT(NP),NP=1,NNP),(THET(NP),NP=1,NNP),
   >(VX(NP),NP=1,NNP),(VZ(NP),NP=1,NNP)
```

***data is read by,

```
    READ(1),TIME,(H(NP),NP=1,NNP),(HT(NP),NP=1,NNP),((TH(M,IQ),
   >M=1,NEL),IQ=1,4),(VX(NP),NP=1,NNP),(VZ(NP),NP=1,NNP)
```

where H and HT are pressure and hydraulic head respectively, TH (or THET) is moisture content, and VX,VZ are horizontal and vertical components of Darcy velocity.

Data Set 4

Dirichlet Boundary Control FORMAT(10I5)

This data set is required only when NBCT > 0 (data set 2). The number of Dirichlet nodes must be specified for each species (radionuclide) in the decay chain (recall NSPEC ≤ 10).

Card	Variable	Column	Format	Definition
1	INBC(1)	1-5	I5	Number of Dirichlet nodes for species 1
	⋮	⋮	⋮	⋮
	INBC(NSPEC)		I5	Number of Dirichlet nodes for species NSPEC

Data Set 5

Cauchy Boundary Control FORMAT (10I5)

This data set is required only when NSTT > 0 (data set 2). The number of Cauchy element sides must be specified for each species (NSPEC ≤ 10).

Card	Variable	Column	Format	Definition
1	INST(1)	1-5	I5	Number of element sides with Cauchy flux boundary condition for species 1
	⋮	⋮	⋮	⋮
	INST(NSPEC)		I5	Number of element sides with Cauchy flux boundary condition for species NSPEC

Data Set 6 Time Integration Parameters FORMAT(8F10.0)

Parameters for controlling the time step sequence are specified in this data set. Time steps may be advanced geometrically up to a maximum value DELMAX, with CHNG as the advancing parameter (i.e., $\Delta t_{n+1} = \Delta t_n(1 + CHNG)$). When transient boundary conditions are requested, (ITRBC=1, Data Set 2) a leach time for band release of the radionuclides may be specified here as TLEACH. When ITRBC=0, (steady boundary conditions) TLEACH is set to TMAX + 1.0 in the code and the input here can be either zero or a blank field. If transient boundary conditions are requested but a leach time is not to be specified, the user should set TLEACH to a value larger than TMAX.

Card	Variable	Column	Format	Definition
1	DELT	1-10	F10.0	Initial time step size, (T)
	CHNG	11-20	F10.0	Multiplier for increasing time step size
	DELMAX	21-30	F10.0	Maximum time step size allowed, (T)
	TMAX	31-40	F10.0	Value of maximum simulation time, (T)
	W	41-50	F10.0	Time derivative weighting; 0.5 = for Crank-Nicolson, 1.0 = for backward difference
	TLEACH	51-60	F10.0	Leach time for radionuclide boundary condition

Data Set 7 — Printed Output Control — FORMAT(80I1)

This data set specifies the timeplanes for which printed output is desired. The print control index refers to the timeplane number ITM. The number of cards required depends on the number of time steps, NTI, according to,

no. of cards = (NTI + 1)/80 + 1

Card	Variable	Column	Format	Definition
1	KPRO	1	I1	Printer control for steady-state and initial conditions; 0 = no print 1 = print mass balance data, 2 = and concentration solutions, 3 = and material fluxes
	KPR(1)	2	I1	
	KPR(2)	3	I1	Similar to KPRO but as a function of time index ITM
	⋮	⋮	⋮	
	KPR(NTI)		I1	

Data Set 8 — Auxiliary Storage and Flow Field Control — FORMAT(80I1)

This data set controls the amount of flow field print output and the timeplanes for which species concentration solutions are stored. The following is stored on logical unit 2 by specifying KDSK(ITM) ≥ 1.

```
      WRITE(2)(TITLE(I),I=1,7),NPROB,NNP,NEL,NBN
      WRITE(2)(NPB(NP),NP=1,NBN)
      DO 5 M=1,NEL
      WRITE(2)(IE(M,IQ),IQ=1,5)
    5 CONTINUE
      WRITE(2)(X(NP),NP=1,NNP)
      WRITE(2)(Z(NP),NP=1,NNP)
      WRITE(2)TIME,ITIM,ISPEC,(R(NP),NP=1,NNP)
```

where NBN,NPB are the number of boundary nodes and the list of global node numbers, respectively, IE,X,Z are local to global node number connectivity arrays and spatial coordinate vectors, respectively, ITIM is the timeplane number, ISPEC is the species number and R contains the nodal values of concentration. The last line is repeated for every timeplane. The number of cards required is the same as in Data Set 7.

Card	Variable	Column	Format	Definition
1	KDSKO	1	I1	Auxiliary storage and flow field print control; 0 = no print, 1 = print flow mass balance data, 2 = and Darcy velocities, 3 = and moisture content field, 4 = and hydraulic head field
	KDSK(1) ⋮ KDSK(NTI)	2 ⋮	I2 ⋮	Similar to KDSKO as a function of time index ITM

==========

Data Set 9 — Material Properties — FORMAT (8F10.0)

This data set specifies material properties for NMAT(NMAT ≤ 10) different materials (see Data Set 2). The following gives an example of inputs required for one material type. A total of NMAT groups of such cards are required. Note the column format for each entry since not every entry in PROP(I,J) is required. The entries not specified here will be in data set 10. The number of entries on each card depends on NMPPM (≤9) from Data Set 2.

Card	Variable	Column	Format	Definition
Group J	PROP(J,2)	11-20	F10.0	Bulk density for material J, (M/L^3)
	PROP(J,3)	21-30	F10.0	Longitudinal dispersivity for material J, (L)
	PROP(J,4)	31-40	F10.0	Transverse dispersivity for material J, (L)

PROP(J,6)	51-60	F10.0	Porosity for material J
PROP(J,7)	61-70	F10.0	Modified coefficient of compressibility of medium J, (L^{-1})
PROP(J,9)	1-10	F10.0	Tortuosity factor for material J

Data Set 10 — Species and Material Dependent Properties — FORMAT(8F10.0)

This data set specifies properties which depend both on species and material type. A total of NSPEC (Data Set 2) groups of NMAT cards is required. The following gives an example of one group of NMAT cards required for species ISPEC ($1 \leq ISPEC \leq NSPEC$).

Card	Variable	Column	Format	Definition
J	SPROP(ISPEC,J,1)	1-10	F10.0	Distribution coefficient for material J and species ISPEC, (L^3/M)
	SPROP(ISPEC,J,2)	11-20	F10.0	Decay constant for species ISPEC in material J, (T^{-1})
	SPROP(ISPEC,J,3)	21-30	F10.0	Molecular diffusion coefficient for species ISPEC in material J, (L^3/T)
	⋮	⋮	⋮	⋮
NMAT	SPROP(ISPEC,NMAT,1)	1-10	F10.0	
	SPROP(ISPEC,NMAT,2)	11-20	F10.0	
	SPROP(ISPEC,NMAT,3)	21-30	F10.0	

Data Set 11 — Nodal Point Coordinates — (I5,2F10.3)

This data set (and the next) is only required if IMESH=0 in Data Set 2. In general, one card is required per node for a total of NNP cards. However, if some nodes fall on a straight line and are equidistant, data for only the first and last points are needed. Intermediate node coordinates are automatically generated by linear interpolation.

Card	Variable	Column	Format	Definition
1	NP	1-5	I5	Node number
	X(NP)	10-15	F10.3	X-coordinate of node NP
	Z(NP)	16-25	F10.3	Z-coordinate of node NP
2	⋮	⋮	⋮	⋮

==========

Data Set 12 Element Connectivity FORMAT(16I5)

This data set is needed only if IMESH=0 in data set 2. In general, one card per element is required for a total of NEL cards. However, for a rectangular block of elements, it is only necessary to specify the first element, and the width and length of the block (i.e., the number of elements in each direction). Subsequent elements to the first in the block will be generated automatically.

Card	Variable	Column	Format	Definition
1	MI	1-5	I5	Element number
	IE(MI,1)	6-10	I5	Global node numbers of element MI
	IE(MI,2)	11-15	I5	beginning with lower left and
	IE(MI,3)	16-20	I5	progressing around element in
	IE(MI,4)	21-25	I5	counter-clockwise direction
	IE(MI,5)	26-30	I5	Material type for element MI
	MODL	31-35	I5	Number of elements in width of block
	NLAY	36-40	I5	Number of elements in length of block
	⋮	⋮	⋮	⋮

Data Set 13 — Material Correction — FORMAT(16I5)

This data set is required only if NCM > 0. Normally, one card is required per material change. However, in those cases where the number of the affected elements ranges from a lower limit of MI to an upper limit of MK with an increment of MINC, automatic correction may be used. Fields MK and MINC are left blank if the automatic generation facility is not used.

Card	Variable	Column	Format	Definition
I	MI	1-5	I5	Element number for which material number is to be corrected
	MTYP	6-10	I5	Corrected material type for element MI
	MK	11-15	I5	Upper limit of automatic correction
	MINC	16-20	I5	Element increment of automatic correction (MK = 0, MINC = 0 for no automatically generated correction)

Data Set 14 — Initial Conditions — FORMAT(I5,5X,F10.0)

Initial conditions must be specified for all NSPEC members in the decay chain being analyzed. The following gives an example for specifying initial conditions for one member. NSPEC such groups of cards are required to specify initial conditions for all chain members. The card groups for each member are entered in the order of the members position in the chain (e.g., data for the first species is entered first). In general, one card per node is required for a total of NNP cards for each species. However, when a sequence of node points have the same initial value, only the upper and lower node values need be specified. The initial concentration for intermediate nodes is taken to be that of the lower bound value.

Card	Variable	Column	Format	Definition
NJ	NJ	1-5	I5	Node number
	RP(NJ)	11-20	F10.0	Initial concentration for Node NJ
		⋮		
	NNP		I5	Final node number
	R(NNP)		F10.0	Initial concentration for node NNP
		⋮		
	data for species 2			
		⋮		
	data for species NSPEC			

==========

Data Set 15 — Dirichlet Boundary Conditions — FORMAT(2I5,F10.0)

This data set is required only if NBCT > 0 (Data Set 2). The following illustrates the input format for one member in an NSPEC membered chain. NSPEC such groups are required, arranged in the same order as the species appear in the chain. In general, one card per Dirichlet node is required for a total of INBC(ISPEC) (Data Set 2) cards for each species. However, if a sequence of Dirichlet nodes are numbered with an increment NPINC, automatic generation may be used. Intermediate node value are set to the value specified on the card for the lower bound node (similar to data set 13). NPINC is set to zero for no automatic generation.

Card	Variable	Column	Format	Definition
NPN	NPN	1-5	I5	Dirichlet node number
	NPINC	6-10	I5	Automatic generation increment to NPN

BB	11-20	F10.0	Dirichlet concentration at node NPN
	⋮		
data for species 2			
	⋮		

Data Set 16 — Neumann Boundary Conditions

The Neumann boundary is the natural boundary condition for the form of the transport equations used here. This condition is the default boundary and need not be specified explicitly.

Data Set 17 — Cauchy Boundary Condition — FORMAT(4I5,5X,4F10.0)

This card is required only if NSTT > 0 (Data Set 2). The following illustrates the specification of one Cauchy element side. In general, INST(ISPEC) such cards are required for each species and NSPEC such groups of cards for the entire decay chain. However, if a sequence of Cauchy elements are numbered with an increment KINC and the node increment is also constant, automatic generation may be used. If a card with KINC > 0 is encountered, the Cauchy elements between the present and previously encountered cards are numbered with a KINC increment and the node point increment on the present card.

Card	Variable	Column	Format	Definition
MPP	NRSE(MP)	1-5	I5	Element number of the element-boundary side, MP
	IS(MP,1)	6-10	I5	First node number of the element-boundary side, MP
	IS(MP,2)	11-15	I5	Second node number of the element-boundary side, MP

KINC	16-20	I5	Automatic generation increment for NRSE
EI	21-30	F10.0	Dot product of flux at node IS(MP,1) with outwardly directed unit vector normal to element-boundary side
EJ	31-40	F10.0	Similar to EI
CI*	41-50	F10.0	Initial concentration at node IS(MP,1) for current species
CJ*	51-60	F10.0	Initial concentration at node IS(MP,2) for current species

⋮

data for species 2

⋮

*The boundary flux is given by $q_3^m = U_i n_i C_1^m$, where the C_1^m depends on the initial concentration in the source fluid (see Equation (10)) and is specified here by the CI, CJ. The initial values are needed when using the Bateman equations for simulating the time-dependent repository condition.

User Supplied Subroutine

When IHYDRO = 1 in Data Set 1 discussed previously, FEMTRAN will access SUBROUTINE HYDRO to be supplied by the user. This subroutine allows space and time specification of the hydrodynamic solution in a general manner. The format for HYDRO is as follows,

```
SUBROUTINE HYDRO (H,HT,TH,VX,VZ,NNP,NEL,X,Z,IE,TIME,MAXEL,MAXNP)
DIMENSION H(MAXNP),HT(MAXNP),TH(MAXEL,4)
DIMENSION VX(MAXEL,4),VZ(MAXEL,4)
DIMENSION X(MAXNP),Z(MAXNP),IE(MAXEL,5)
.
.
.
FORTRAN code to generate hydrodynamic solution
.
.
.
RETURN
END
```

Where the variables in the subroutine parameter list are:

H(NP): vector containing nodal values of pressure head at time TIME.

HT(NP): vector containing nodal values of hydraulic head at time TIME.

TH(M,IQ): an array containing elemental values of moisture content for all elements (M = 1, NEL) and for each local node value (IQ = 1,4) at time TIME.

VX(M,IQ),VZ(M,IQ): arrays containing elemental values of Darcy velocity for all elements (M = 1,NEL) and for each local node (IQ = 1,4) at time TIME.

NNP: the number of node points for problem.

NEL: the number of elements for problem.

X(NP),Z(NP): vectors containing the spatial coordinates x,z, as a function of node point NP.

IE(M,IQ): an array containing the local to global node connectivities for element M, i.e., IE(M,IQ) contains the global node number for element M at local node IQ (recall that local node numbers proceed in a counter-clockwise direction about the element starting at the lower left corner).

TIME: current computational time.

MAXEL: maximum number of elements allowable due to program dimensions (MAXEL = 1200 currently).

MAXNP: maximum number of node points allowable due to program dimensions (MAXNP = 1300 currently).

Job Control Cards

The code FEMTRAN is maintained in UPDATE format in the Sandia National Laboratories (SLA) permanent file system. Although the present version of FEMTRAN executes on the CRAY-1S computer, machine dependent code was avoided such that FEMTRAN will execute on other machines with minimal modifications. The following discussion of job control language refers to the use of FEMTRAN on the SLA computer system.

Because FEMTRAN is maintained in UPDATE format, the file must be attached, run through the UPDATE processor and compiled prior to execution. Several example control streams are presented in the following to illustrate the use of FEMTRAN under various modes of operation. Figure 3 shows the control stream format when no peripherals are required for execution. This example represents a run with an internally specified mesh (IMESH = 0) and a hydrodynamic solution generated with user subroutine HYDRO discussed in the previous section. An example of an execution with mesh and hydrodynamic solution read from disk files is given in Figure 4. Also shown in the figure are the commands to divert the auxiliary storage file (logical unit 2), which may be used for post processing of solutions, and commands to request microfiche of all output.

```
JOBNAME,TXXX,STSCZ.                                    NAME     BOX NO.
USER . . . .
CHARGE . . . .
SLTLIB.
UID.        NAME   BOX NO.
CUPDATE,P=FEMTRNC,UN=MJMARTI,F.
CFT(I=COMPILE,ON=AZ,L=0)
LDR.
7-8-9
IDENT,USERSUB
*DELETE,FEMTRANC.1112,FEMTRANC.1117
     FORTRAN code for SUBROUTINE HYDRO
7-8-9
     FEMTRAN DATA
6-7-8-9
```

Figure 3. Job Control Stream -- Running With User Subroutine.

```
JOBNAME,TXXX,STSCZ.                                NAME     BOX NO.
USER . . . .
CHARGE . . . .
SLTLIB.
UID.       NAME    BOX NO.
ACCESS,DN=FT01,PDN=file name,ED=XX,UQ.
ACCESS,DN=FT09,PDN=file name,ED=XX,UQ.
REWIND,DN=FT01:FT09.
CUPDATE,P=FEMTRNC,UN=MJMARTI,F.
CFT(I=COMPILE,ON=AZ,L=0)
LDR.
DISPOSE,DN=FT02,SDN=PLT1,DC=ST,DF=TR,^
TEXT='CTASK.ROUTE,PLT1,DC=PU,TID=XX.'.
REWIND,DN=$OUT.
COPYD,I=$OUT,O=FOUT.
XFICHE,FOUT,T='JOB TITLE'.
7-8-9
7-8-9
     FEMTRAN DATA
6-7-8-9
```

Figure 4. Job Control Stream -- Running with Disk Files.

V. SAMPLE PROBLEMS

Three sample problems are presented in this chapter to demonstrate the capabilities of FEMTRAN and to illustrate the preparation of the input stream for execution. Although the problems were chosen to illustrate various features of the code, all possible options could not be covered. An effort was made, however, to cover features that would seem the most difficult to master from reading the text alone.

1. One-Dimensional Transport -- Cauchy Boundary Condition

This problem was selected to illustrate the use of user specified mesh generation, hydrodynamic solution, and the transient flux boundary condition features of the code. It also provides a comparison with the analytic solution given in References 19 and 20. The problem involves the transport of a three-member radionuclide decay chain through a saturated, homogeneous, rigid porous medium. The flow field is uniform and specified as 239.4 ft/yr. The parameters are given in Tables 2 and 3 and the input stream is also shown in Figure 5. The initial condition assumes zero concentration in the computational region for all members. The inlet boundary conditions are given by,

$$u_x C^m - D_{xx} \frac{\partial C^m}{\partial x} = u_x C_1^m \quad , \quad x = 0$$

Table 2. Radionuclide Properties

Component, n	Half-life $t_{1/2}$ (yr)	Retention Factor R_d^m	Initial Inventory C_o^m
1	433	9352	1
2	15	9352	0
3	6540	9352	0

```
001 LESTER'S PROBLEM
156  077   01    0   42   00    3    1    1    1    8    0    0    0
  3    1    0    0    0    1
  1    1    1
    9 10        0.0        9.1      273.9       0.3      300.
3100020100201001010020100101022000000000020000000003000000000300000000003000000000
1100000001000000000010000000001000000000010000000001000000000010000000001000000000
  0.0        1.00      008.3      0000.0                0.1        0.
   935.1      .0016      0.0
   935.1      .0462      0.0
   935.1    .000106      0.0
 01          0.          0.
  6          3.          0.
  7          0.          1.
 12          3.          1.
 13         7.3          0.
 18         20.          0.
 19         7.3          1.
 24         20.          1.
 25         25.          0.
 29         45.          0.
 30         35.          1.
 34         45.          1.
 39         70.          1.
 40         90.          0.
 49         95.          0.
 50         75.          1.
 55        100.          1.
 56        100.          0.
 61        150.          0.
 62        110.          1.
 71        200.          1.
 72        140.          0.
 81        230.          0.
 82        210.          1.
 91        300.          1.
 92        260.          0.
101        350.          0.
102        310.          1.
111        400.          1.
112        360.          0.
121        450.          0.
122        410.          1.
131        500.          1.
132        460.          0.
136        500.          0.
137        550.          0.
141        750.          0.
142        550.          1.
151       1000.          1.
152        800.          0.
156       1000.          0.
 01    .1    2   08   07    1   05    1
  6     6   13   19   12    1    1    1
  7    13   14   20   19    1    3    1
 12    18   25   30   24    1    1    1
 13    25   26   31   30    1    4    1
 17    29   40   35   34    1    1    1
 18    40   41   36   35    1    4    1
 22    44   45   50   39    1    1    1
 23    45   46   51   50    1    4    1
 27    49   56   55   54    1    1    1
 28    56   57   62   55    1    1    1
 29    57   58   63   62    1    4    1
 33    61   72   67   66    1    1    1
 34    72   73   68   67    1    4    1
 38    76   77   82   71    1    1    1
 39    77   78   83   82    1    4    1
 43    81   92   87   86    1    1    1
 44    92   93   88   87    1    4    1
 48    96   97  102   91    1    1    1
 49    97   98  103  102    1    4    1
 53   101  112  107  106    1    1    1
 54   112  113  108  107    1    4    1
 58   116  117  122  111    1    1    1
 59   117  118  123  122    1    4    1
 63   121  132  127  126    1    1    1
 64   132  133  128  127    1    4    1
 68   136  137  142  131    1    1    1
 69   137  138  143  142    1    4    1
 73   141  152  147  146    1    1    1
 74   152  153  148  147    1    4    1
  1          0.0
156          0.0
  1          0.0
156          0.0
  1          0.0
156          0.0
  1    1    7    0     239.4       239.4        1.        1.
  1    1    7    0      0.0         0.0         0.        0.
  1    1    7    0      0.          0.          0.        0.
```

Figure 5. Input Data Deck for Sample Problem 1

Table 3. Transport Parameters

Darcy velocity, u_x	239.4	ft/yr
connected porosity, ϕ	0.1	
dispersivity, a_L	8.5	ft
dispersion coefficient, D_{xx}	2035.0	ft^2/yr

where the C_1^m are given by the Bateman equation presented in Equation (10). The outlet boundary condition for the analytic problem assumes a semi-infinite region. This is approximated by the Neumann boundary condition specified at 1000 ft from the inlet for the numerical solution. The computational mesh consisted of a row of 77 four node quadrilateral elements of variable length. Element lengths varied from 1 foot at the inlet to 50 feet beyond 500 feet from the inlet. All elements were 1 foot wide. The data cards for specifying this mesh are shown in Figure 5. The simulation was carried out to 273 years by specifying a constant 9.1 year time step. The comparison between the numerical and analytical solution is shown in Figure 6. The comparison is good despite the rather coarse time step relative to the short half-life of nuclide 2. The cumulative mass balance history is given in Figure 7 for the three nuclides. The ordinate values in Figure 7 are described as follows. Define,

$$DIV^m = \int_o^t \int_B \left(u_i C^m - D_{ij}^m \frac{\partial C^m}{\partial x_j}\right) n_i \, dB \, dt$$

$$ACM^m = \int_o^t \int_B \frac{\partial}{\partial t}(\theta C^m) + \frac{\partial}{\partial t} \rho S^m + \lambda^m \theta R_d^m C^m - \lambda^{m-1} \theta R_d^{m-1} C^{m-1} \, dR \, dt$$

then the percent difference between divergence and accumulation functions is defined by,

$$\text{Percent Difference} = \frac{DIV^m - ACM^m}{ACM^m} \times 100$$

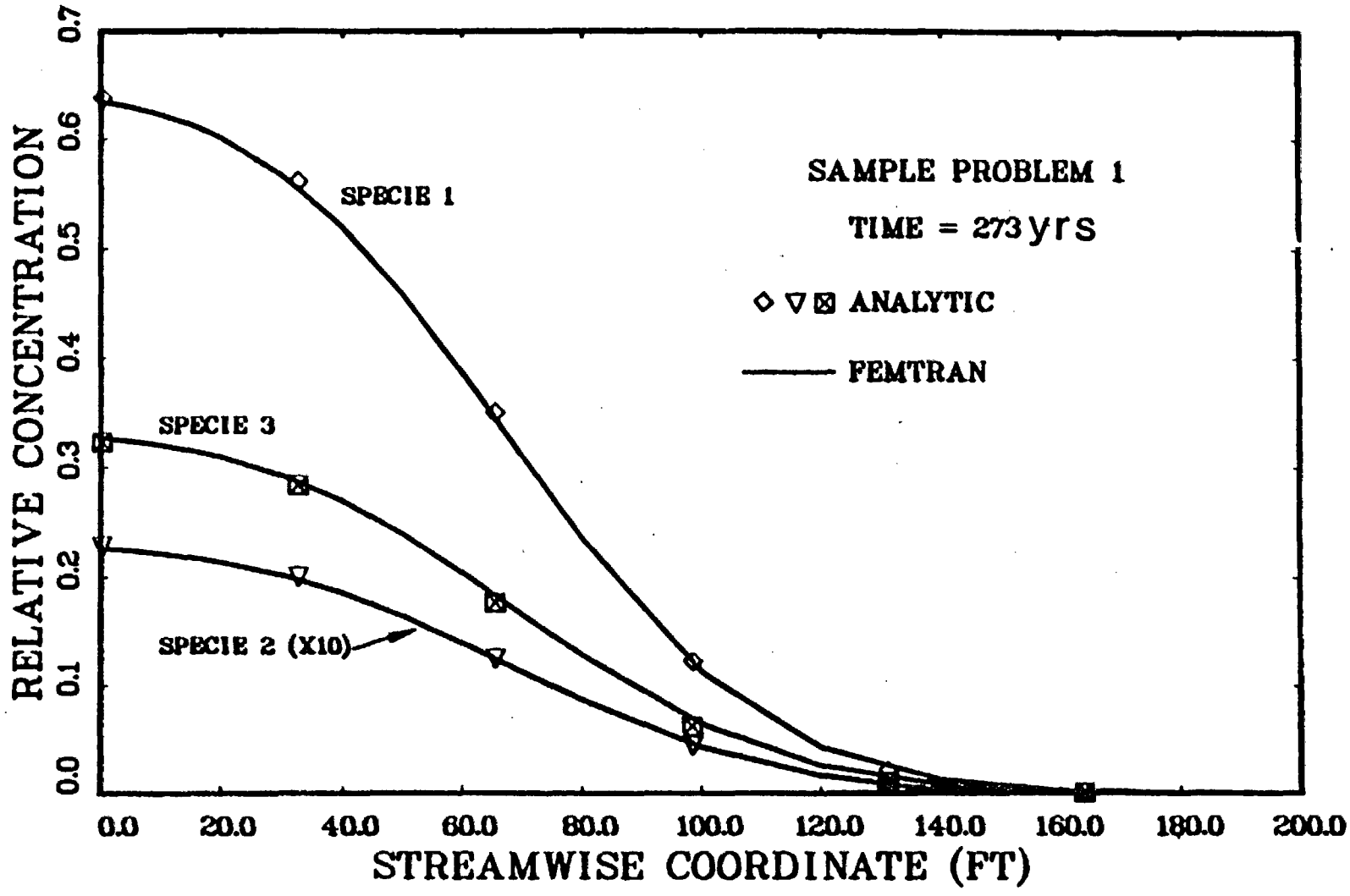

Figure 6. Comparison Between Numerical (FEMTRAN) and Analytical (Ref. 20) Solutions of Relative Concentration Profiles at 273 Years

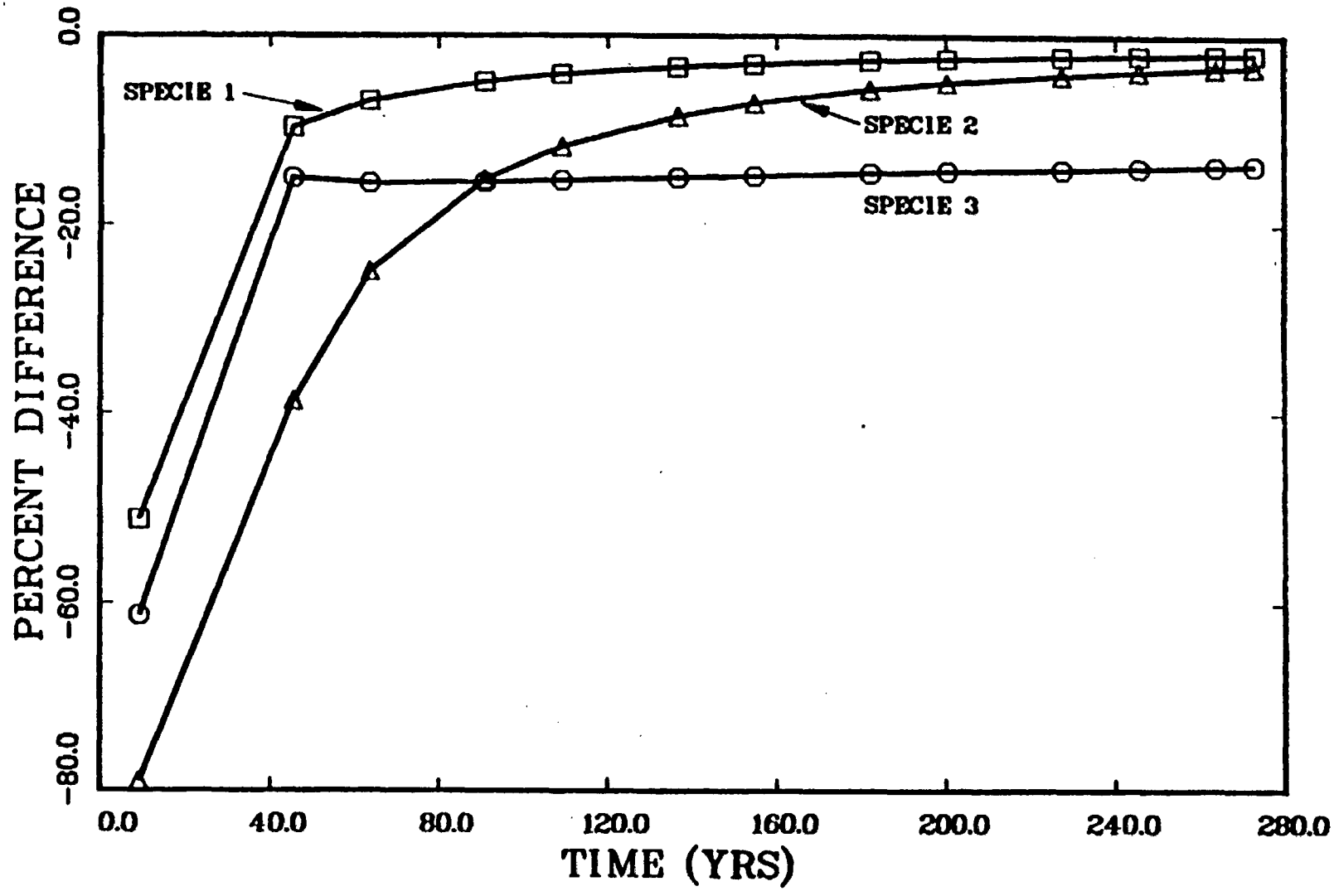

Figure 7. Cumulative Mass Balance History for Sample Problem 1

The mass balance results indicate that most of the error occurs early in the simulation and decreases with time. This is not surprising since the boundary condition represents a mathematical discontinuity at the inlet. The error is a few percent over most of simulation for nuclides 1 and 3. The larger percent difference for nuclide 2 can be attributed to the contrast in half-life with its precursor nuclide 1, and the rather coarse time steps which are close to the half-life value (9.1 vs. 15 yr). The mass balance computations shown in Figure 7 are part of the FEMTRAN output and are useful indicators of the accuracy and consistency of computed solutions.

2. One-Dimensional Transport -- Dirichlet Boundary Condition

Problem 2 describes the one-dimensional transport of a three-member decay chain through a saturated sorbing porous medium. The problem is similar to problem 1 only in geometry, otherwise the transport parameters are quite different. The source of radionuclides is described by the Dirichlet boundary condition. This problem, and the next, have been investigated in the INTRACOIN[21] study. The INTRACOIN (International Nuclide TRAnsport COde INtercomparison study) is a benchmarking study designed to assess numerical methods used by various countries for prediction of radionuclide transport by intercomparison of their respective solutions to selected problems. Parameters for the problems are chosen to provide a rigorous test of the computational method. Sample problem 2 described here represents INTRACOIN level 1, case 1, variation (I1, T2, B1, L1, P2, R2). The variation parameters are defined as follows.

Table 4. I1: Long-lived Parent Nuclide

Nuclide	m	$t_{1/2}$ (yr)	$I^m(o)$
^{234}U	1	2.445 E+5	1.000
^{230}Th	2	7.7 E+4	0.010
^{226}Ra	3	1.600 E+3	0.004

$I^m(o)$ in Table 4 denotes the initial activity ratio of the m-th nuclide normalized by the initial activity of ^{234}U. The nuclide half-lives are denoted by $t_{1/2}$.

T2: Leach duration for nuclide sources.

$T = 10^5$ yrs

B1: Dirichlet Boundary condition at source.

$N^m(o,t) = I^m(t)/QT$

where $Q = 1\ m^3/yr$, $T = 10^5$ yr. $N^m(o,t)$ denotes the activity of nuclide m at the boundary.

L1: Distance from source to observation point.

$\ell = 500$ m

P2: Peclet number based on problem length ℓ.

$Pe = \ell/a_L = 10$ (a_L longitudinal dispersivity)

R2: Retention factor set 2.

$R_d^m = 1 + \rho K_d^m/\phi$, ϕ denotes matrix porosity

Table 5. Retention Factors

Nuclide m		R_d^m
^{234}U	1	60
^{230}Th	2	500
^{226}Ra	3	20

The interstitial ground water velocity, v, is specified as 1 m/yr and the porosity as 10%. The mesh and outlet boundary condition used in this problem are identical to that of Problem 1 (note that the units are meters here). The input stream for this problem is shown in Figure 8. The initial time step was set to 121 years and increased geometrically to 2000 years with a 10% increase at each time step. The time step was increased to 5000 years for times greater than 200,000 years and again to 10,000 years for times greater than 500,000 years. The calculation was carried out to 10^6 years.

```
 002  INTRACOIN BENCHMARK CASE 1 (I1,T2,B1,L1,P2,R2)
 156   77   01    0  233   06    0    1    1    1    7    0    0    0
   3    1    0    0    0    1
   2    2    2
  121 589        0.1      2000.   1001000.        0.9    1.0E09
210000000100000000020000200002000000000200000000020202200002000020000200000000
20         2         2         2         2         2         2         2
2          2         2         2         2         2         2         2
4                    1    1    1         1         1 1 11    1    1    1
1          1         1         1         1         1         1         1
1          1         1         1         1         1         1         1
    0.0          1.          50.         0.        0.          .01        0.    0.
      0.59  2.835E-6         0.0
      4.99    9.0E-6         0.0
      0.19  4.332E-4         0.0
   01         0.        0.
    6         9.        0.
    7         0.        1.
   12         9.        1.
   13        7.9        0.
   18        20.        0.
   19        7.9        1.
   24        20.        1.
   25        25.        0.
   29        45.        0.
   30        25.        1.
   34        45.        1.
   39        70.        1.
   40        50.        0.
   49        95.        0.
   50        75.        1.
   55       100.        1.
   56       100.        0.
   61       150.        0.
   62       110.        1.
   71       200.        1.
   72       140.        0.
   81       250.        0.
   82       210.        1.
   91       300.        1.
   92       260.        0.
  101       350.        0.
  102       310.        1.
  111       400.        1.
  112       360.        0.
  121       450.        0.
  122       410.        1.
  131       500.        1.
  132       460.        0.
  136       500.        0.
  137       550.        0.
  141       750.        0.
  142       550.        1.
  151      1000.        1.
  152       900.        0.
  156      1000.        0.
   01    1    2   08   07    1   03    1
    6    6   13   19   12    1    1    1
    7   13   14   20   19    1    9    1
   12   18   25   30   24    1    1    1
   13   25   26   31   30    1    4    1
   17   29   40   35   34    1    1    1
   18   40   41   36   35    1    4    1
   22   44   45   50   39    1    1    1
   23   45   46   51   50    1    4    1
   27   49   56   55   54    1    1    1
   28   56   57   62   55    1    1    1
   29   57   58   63   62    1    4    1
   33   61   72   67   66    1    1    1
   34   72   73   68   67    1    4    1
   38   76   77   82   71    1    1    1
   39   77   78   83   82    1    4    1
   43   81   92   87   86    1    1    1
   44   92   93   88   87    1    4    1
   48   96   97  102   91    1    1    1
   49   97   98  103  102    1    4    1
   53  101  112  107  106    1    1    1
   54  112  113  108  107    1    4    1
   58  116  117  122  111    1    1    1
   59  117  118  123  122    1    4    1
   63  121  132  127  126    1    1    1
   64  132  133  128  127    1    4    1
   68  136  137  142  131    1    1    1
   69  137  138  143  142    1    4    1
   73  141  152  147  146    1    1    1
   74  152  153  148  147    1    4    1
    1          0.0
  156          0.0
    1          0.0
  156          0.0
    1          0.0
  156          0.0
    1    0        1.0
    7    0        1.0
    1    0  3.07E-03
    7    0  3.07E-03
    1    0 2.486E-03
    7    0 2.486E-03
```

Figure 8. Input Data Deck for Sample Problem 2

The "breakthrough" activity history at the 500 m observation point for the three members is shown in Figure 9. Also shown is the solution generated with the Swedish code RANCH.[22] RANCH is based on a classical one-dimensional advective-dispersive radionuclide model for saturated porous media. The initial inventories defined in the INTRACOIN study are in arbitrary units of activity ratio as are the output results. FEMTRAN computes in units of mass concentration. The following relation was used to convert activity ratios to mass concentration ratios,

$$\frac{C^m}{C^{m-1}} = \frac{N^m}{N^{m-1}} \frac{M^m}{M^{m-1}} \frac{t^m_{1/2}}{t^{m-1}_{1/2}}$$

where M^m denotes atomic weight and the remaining symbols are defined as before. The comparison between the RANCH and FEMTRAN solutions is good over the entire range of activities varying over six powers of ten. The mass balance results for the computation are given in Figure 10. As before, most error occurs early in the simulation reflecting the numerical approximation to the initially discontinuous boundary condition. The band release boundary condition is also discontinuous when $t = T_{leach}$ where the source concentrations are stepped down to zero. The error for ^{234}U increases from the leach time on as the nuclide is transported out of the region. The least error is computed for ^{230}Th which is strongly sorbed resulting in an effective transport velocity given by,

$$v^{Th}_{eff} = \frac{u_x}{\phi R^{Th}_d} = 1/500 \text{ m/yr}$$

The error increases for the faster running nuclides ^{234}U and ^{226}Ra with effective transport velocities of 1/60, 1/20 m/yr, respectively. Improved mass balance results could be obtained at the expense of taking more time steps.

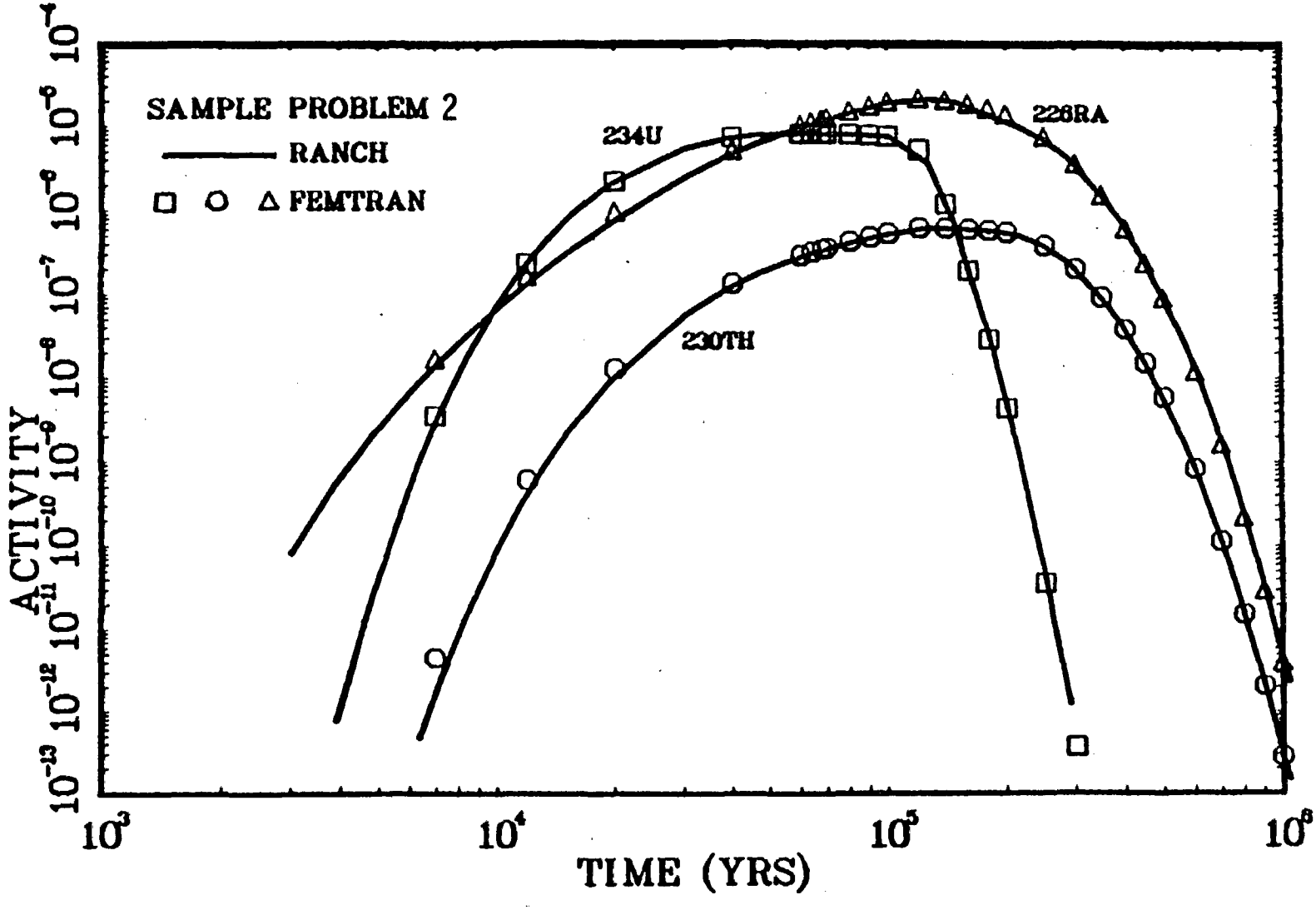

Figure 9. Activity History at 500 m from Source for Sample Problem 2

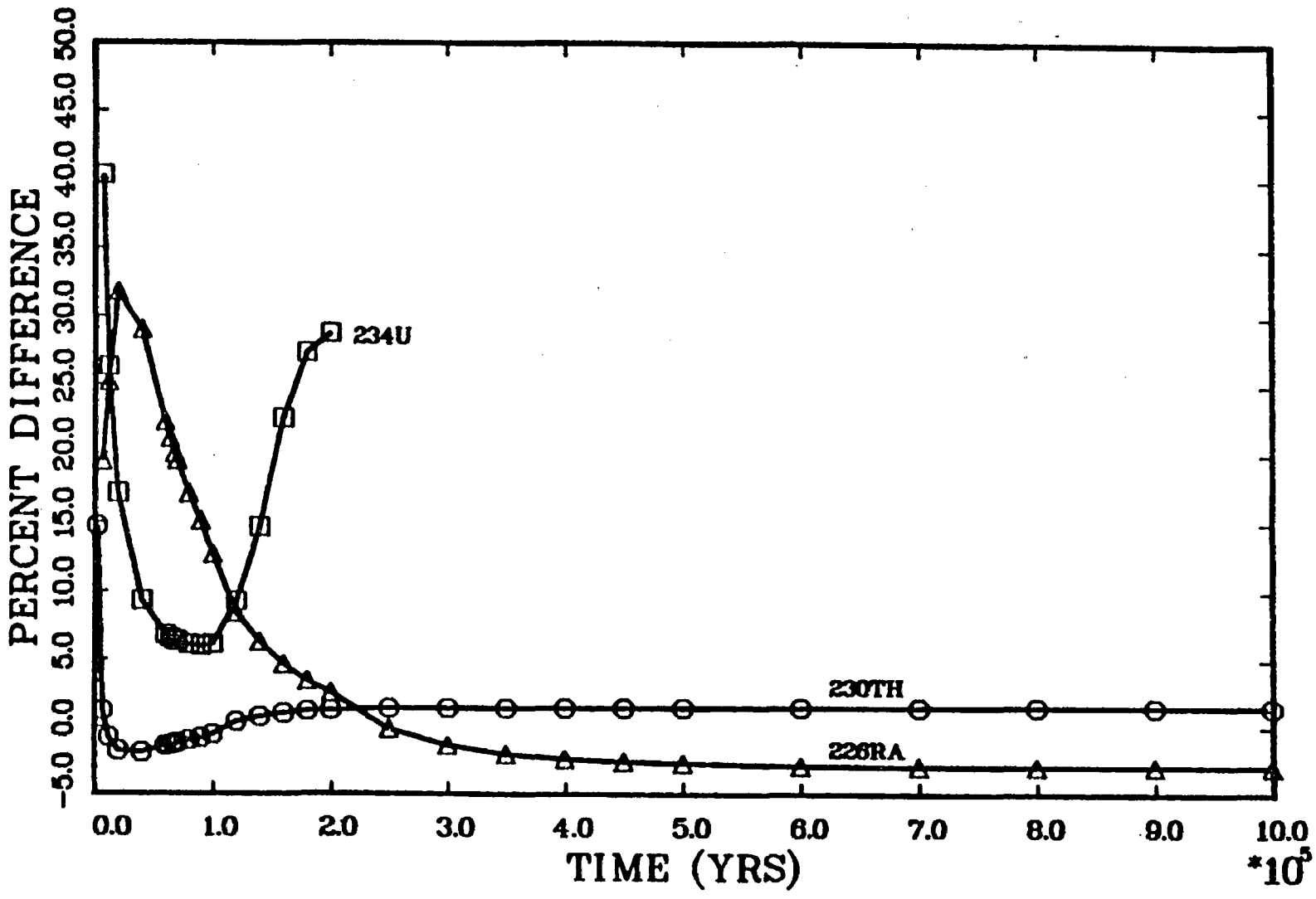

Figure 10. Cumulative Mass Balance History for Sample Problem 2

3. Two-Dimensional Transport -- Dirichlet Boundary Condition

This problem corresponds to INTRACOIN level 1, case 4A, and is essentially the two-dimensional version of problem 2. The nuclide source for this case is defined as a 10 m^2/m slab source placed in the cross stream direction to the uniform flow. Invoking symmetry, only the region $z \geq 0$, $0 \geq x \geq 600$ m is modeled (the flow is in the positive x direction). The finite element mesh for this problem was generated with QMESH[16] and is shown in Figure 11. The mesh data for 608 elements and 660 node points is read in from logical unit 9 as indicated by Data Set 1 and the absence of Data Sets 11 and 12 in the input stream shown in Figure 12. The Dirichlet condition is specified over $x = 0$, $0 \geq z \geq 5$ and the Neumann condition (equation 7) over the remainder of the boundary. The parameters for this problem are identical to those of problem 2 with the addition of transverse dispersivity, a_T, of 5 m. The breakthrough at the 500 m observation point is given in Figure 13 for the three members. Also shown for comparison is the breakthrough from the one-dimensional version, problem 2. The inclusion of transverse dispersion has a significant effect in mitigating the activity at the observation point. The time to maximum breakthrough activity, T_{max}, and the maximum activity, N_{max}, for problems 2 and 3 are summarized in Table 6 as approximated from the output timeplanes for the simulations.

Table 6. Maximum Activity

Nuclide	m	Prob 2 (Case 1) T_{max}(yr)	Prob 2 (Case 1) N_{max}	Prob 3 (Case 4A) T_{max}(yr)	Prob 3 (Case 4A) N_{max}
^{234}U	1	6.00×10^4	0.815×10^{-5}	1.00×10^5	0.440×10^{-5}
^{230}Th	2	1.20×10^5	0.619×10^{-6}	1.4×10^5	0.335×10^{-6}
^{226}Ra	3	1.20×10^5	0.215×10^{-4}	1.4×10^5	0.102×10^{-4}

The profiles of activity ratio along the cross-stream coordinate ($x = 500$ m, $0 \leq z \leq 350$ m) at the times of maximum breakthrough (T_{max} in Table 3) are given in Figure 14. Contours of activity ratio are plotted in Figures 15,

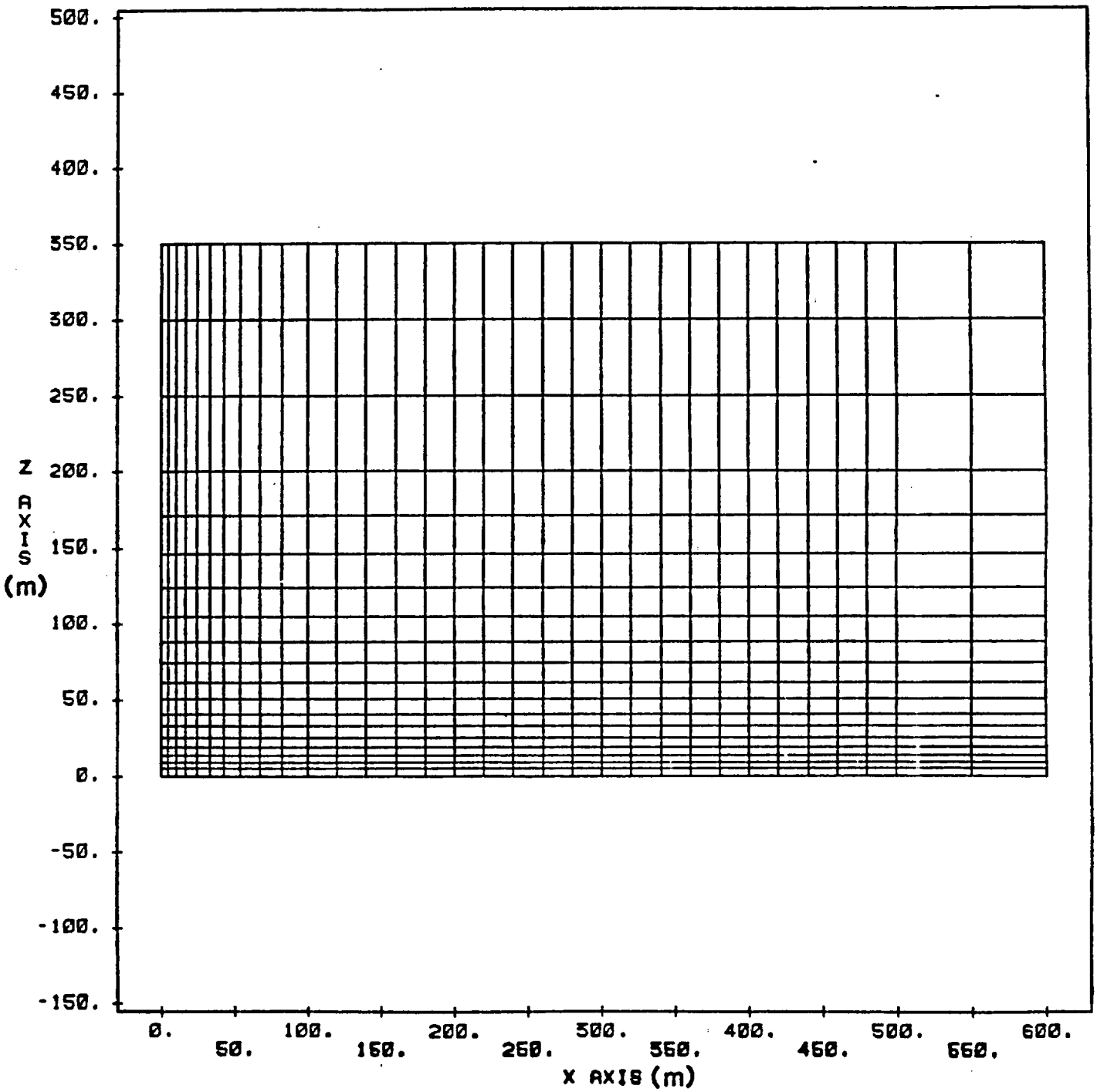

Figure 11. Finite Element Mesh Used for Sample Problem 3 (generated with QMESH[16])

```
 003  INTRACOIN BENCHMARK CASE-4A (I1,T2,B1,L1,P2,R2)
 660  608   01    0  235   06    0    1    1    1    7    0    0    0
   3    1    1    0    0    1
   2    2    2    0
  121.585       0.1     2000.   201000.        0.5    1.0E05
2100000000000000000200002000020000000002000000000202200002000020000200000000
20        2         2         2         2         2         2         2
2         2         2         2         2         2         2         2
4                   1    1    1         1         1 1 11    1    1    1
1         1         1         1         1         1         1         1
1         1         1         1         1         1         1         1
      0.0        1.        50.        5.        0.        .01        0.    0.
     0.59.000002835        0.0
     4.99.000009           0.0
      .19.00043322         0.0
   1          0.0
 660          0.0
   1          0.0
 660          0.0
   1          0.0
 660          0.0
   1    0        1.0
   2    0        1.0
   1    0  3.07E-03
   2    0  3.07E-03
   1    0 2.486E-05
   2    0 2.486E-05
```

Figure 12. Input Data Deck for Sample Problem 3

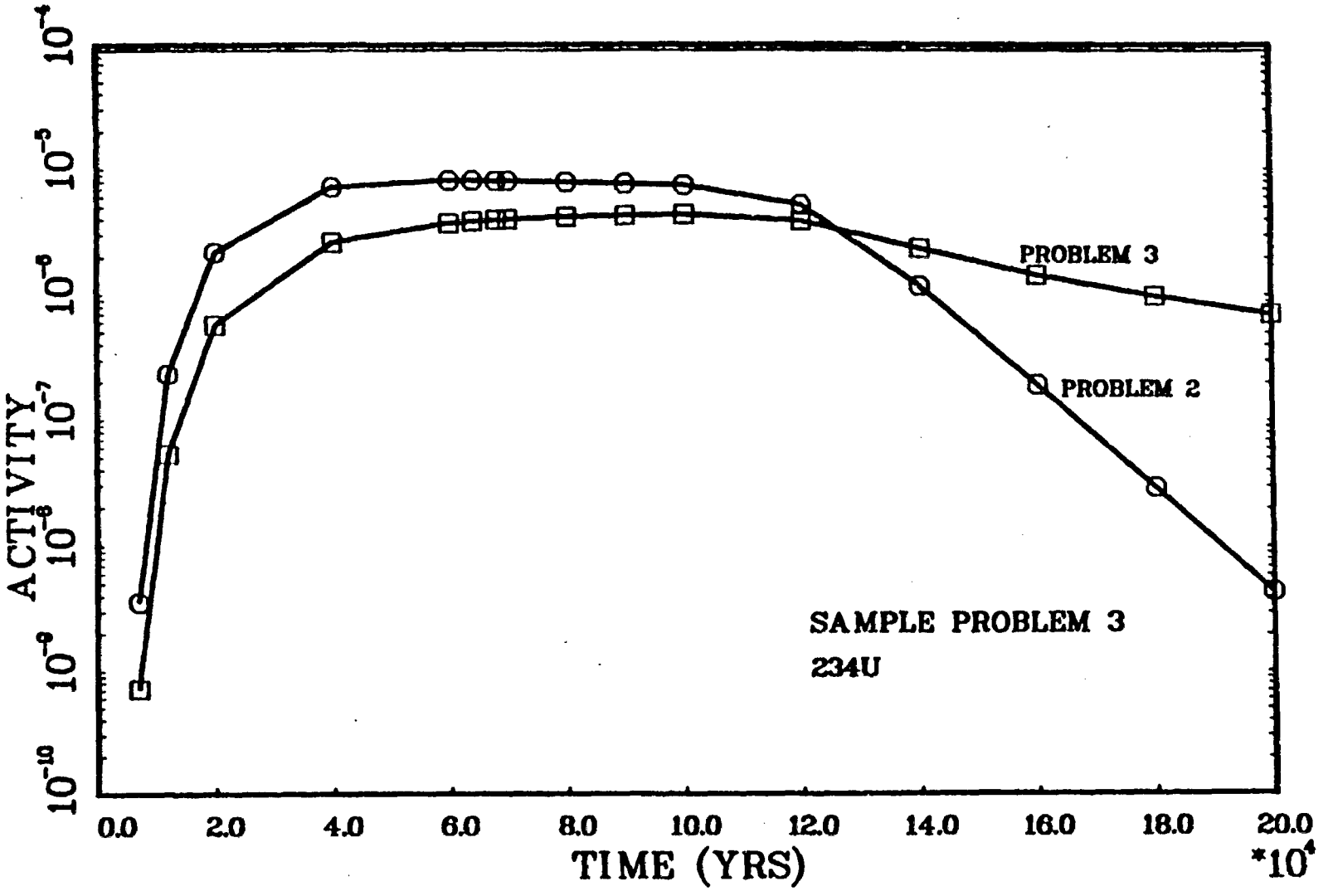

Figure 13a. Activity History at x = 500 m, z = 0 for Sample Problem 3 (results from Problem 2 are also shown for comparison)

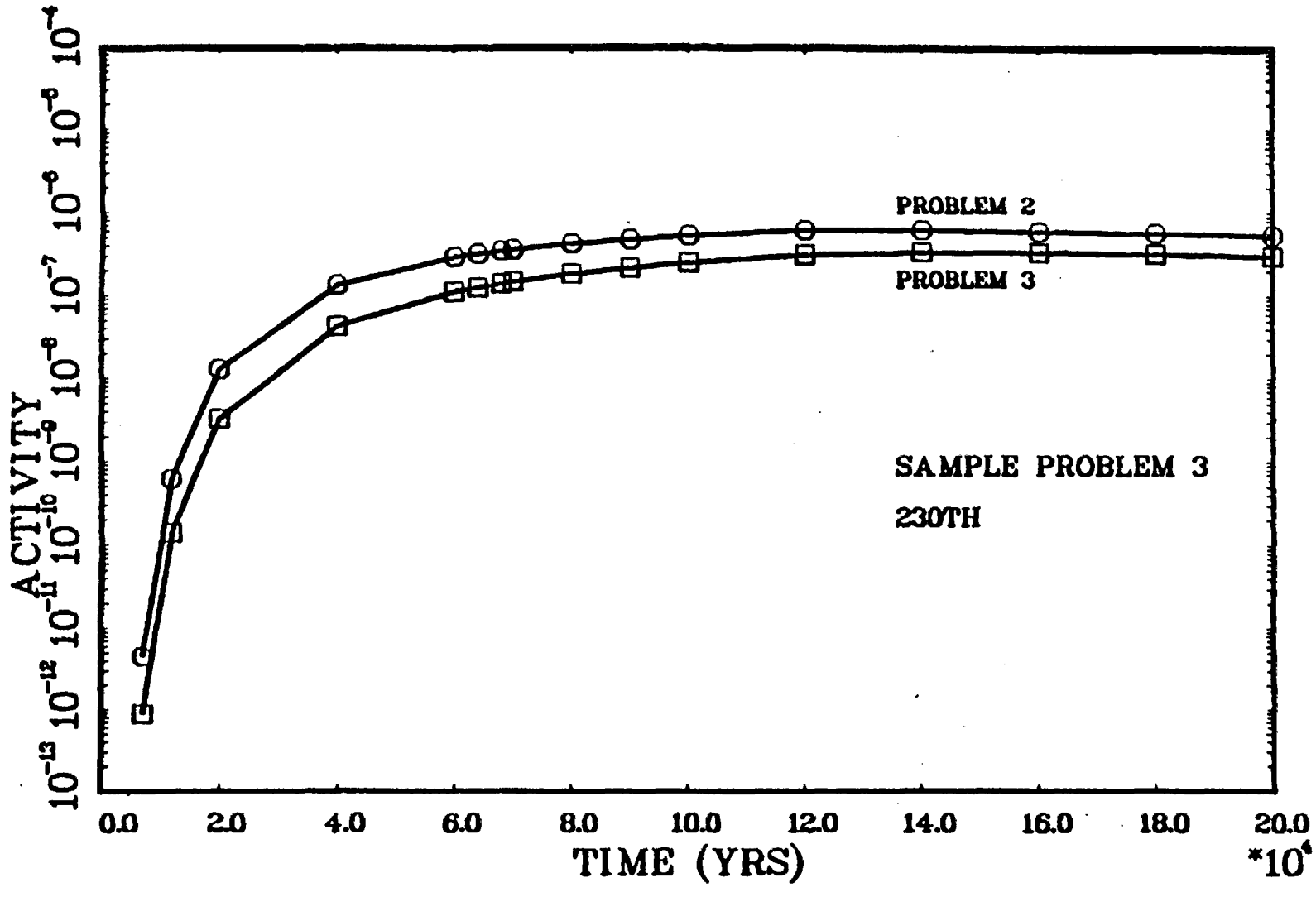

Figure 13b. Activity History at x = 500 m, z = 0 for Sample Problem 3 (results from Problem 2 are also shown for comparison)

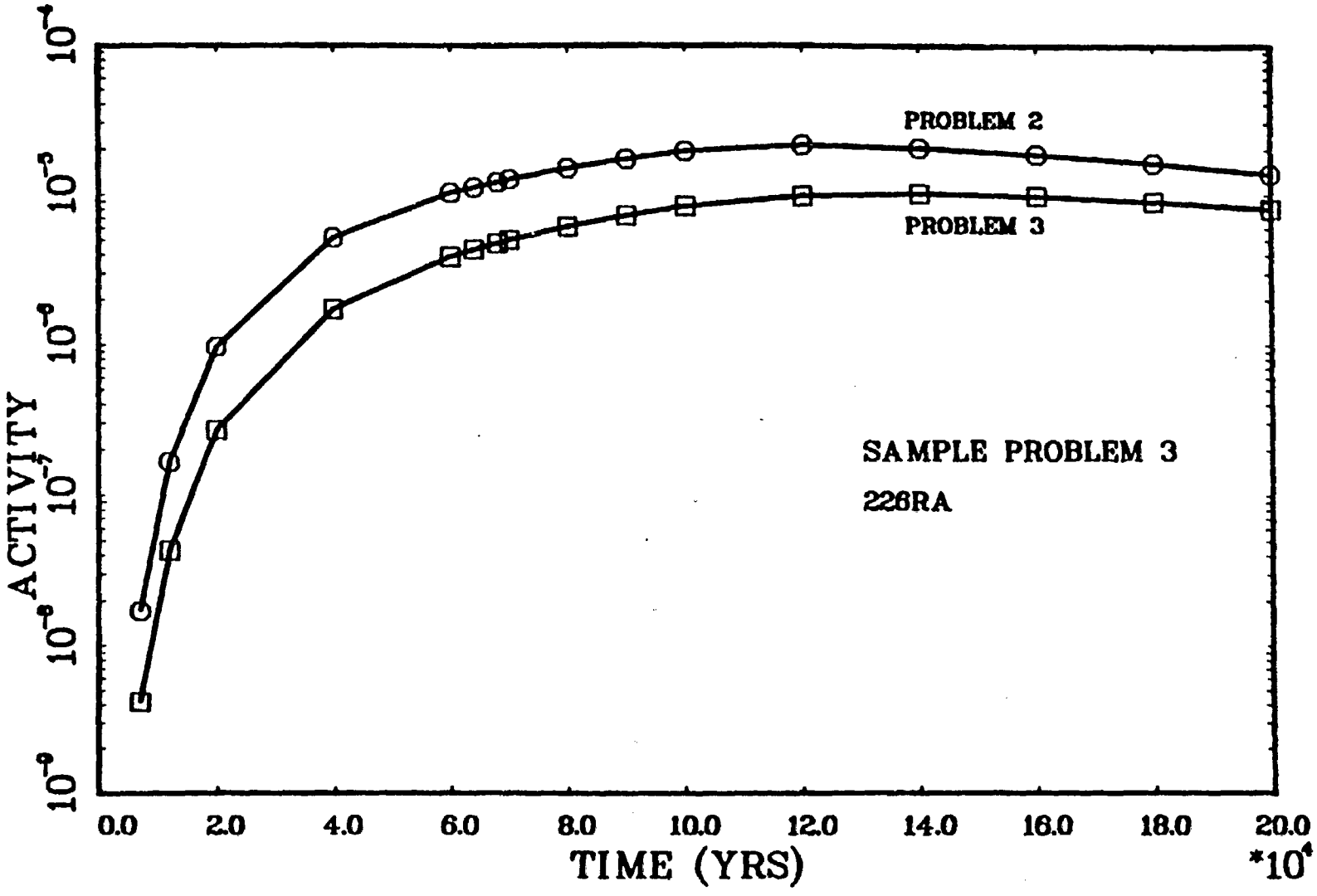

Figure 13c. Activity History at x = 500 m, z = 0 for Sample Problem 3 (results from Problem 2 are also shown for comparison)

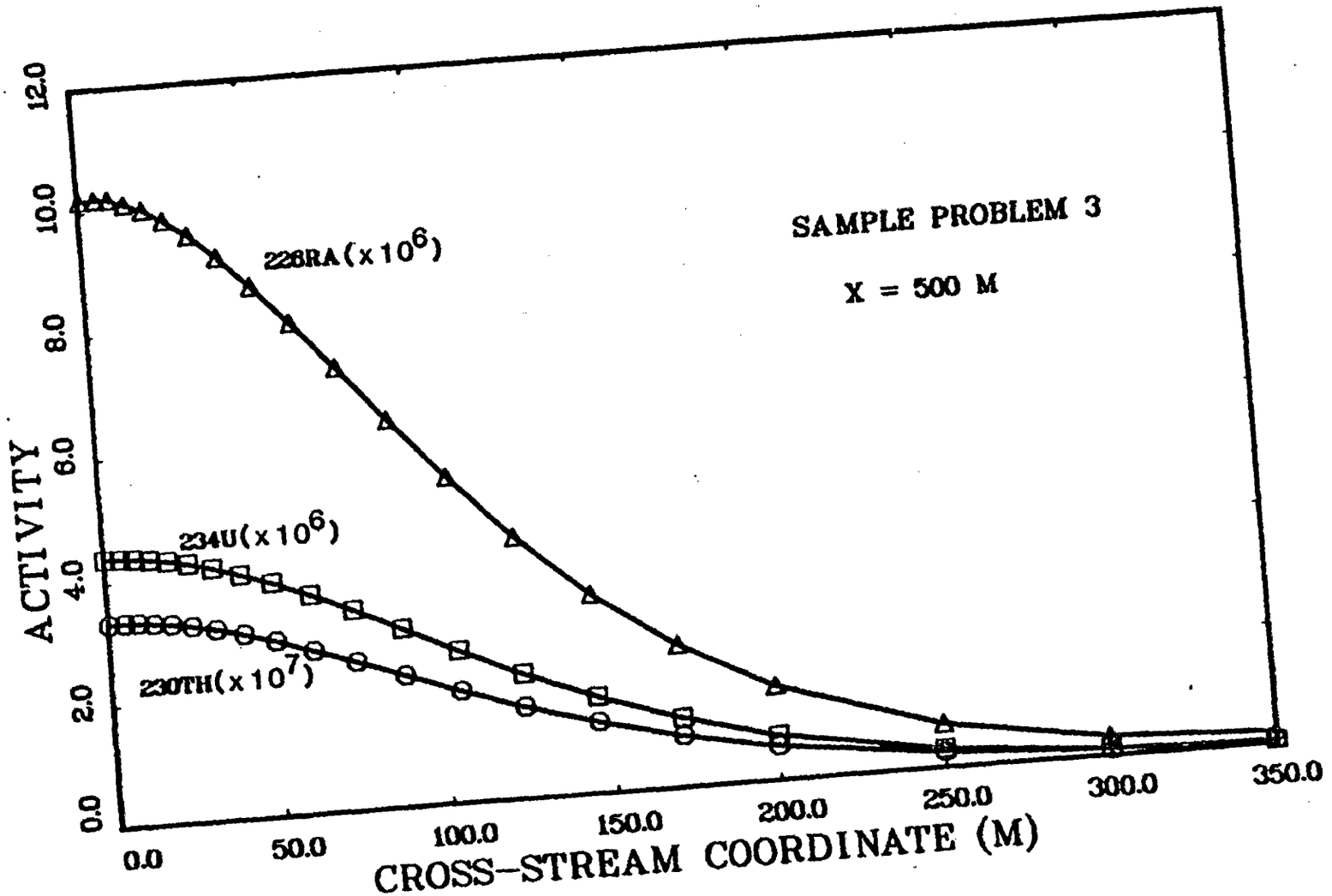

Figure 14. Activity Profiles Along x = 500 m for Sample Problem 3. The time for each profile is at maximum breakthrough activity (see Table 3).

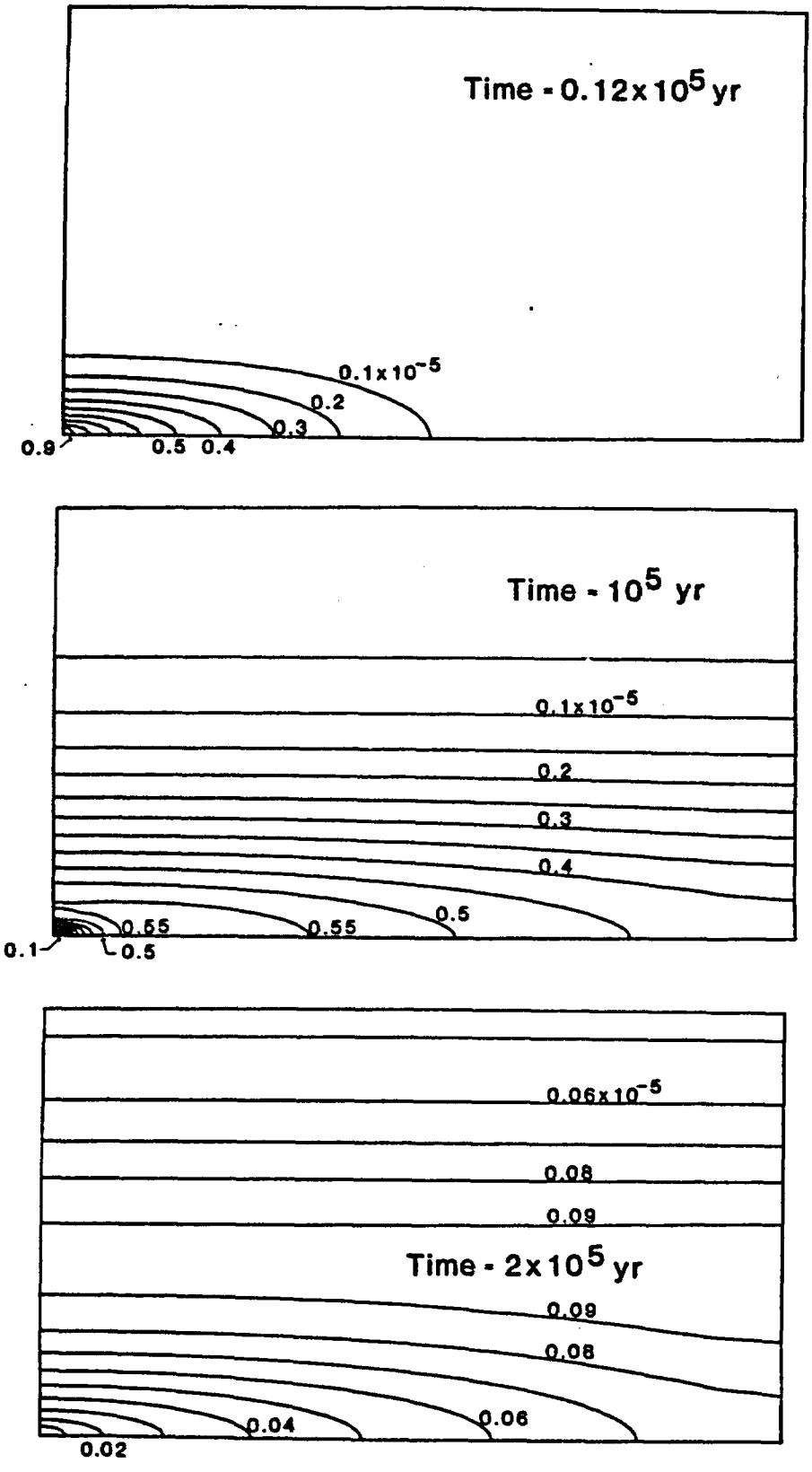

Figure 15. Contours of Activity for ^{234}U -- Sample Problem 3

16 and 17 at times selected to illustrate the overall solution. Contours over the entire 600 x 350 m mesh are plotted. Contours at 0.12 x 10^5 years show the ^{234}U has been transported furthest while the ^{230}Th remains in the immediate vicinity of the source. The results are consistent with the retention factors and effective transport velocities discussed in Problem 2. The effect of the contrast in retention factors, and consequently transport mobility, is even more pronounced at 1.0 x 10^5 years. Figures 15b through 17b show significant transport over the entire length of mesh for ^{234}U and ^{226}Ra while the ^{230}Th remains confined to the vicinity of the source. Also note a maximum activity occurs along the z = 0 line at this time due to the band release boundary condition at the source. This condition persists for ^{230}Th and ^{226}Ra in the 2 x 10^5 year plot. The maximum activity for ^{234}U occurs along the x = 600 m line as the nuclide is transported out of the region. The difference in distribution between ^{234}U and ^{226}Ra, both of which have large mobilities (effective velocity), is the strong coupling of ^{226}Ra to its precursor. The result is a distribution similar to that of ^{230}Th rather than ^{234}U.

The cumulative mass balance history, as defined in Problem 1, is shown in Figure 18 for all three nuclides. As in previous mass balance results, most of the error occurs early in the simulation and decreases with time. The mass balance curve for ^{226}Ra shows the most error which can be attributed to the coarse time steps taken relative to its half-life and retention factor. Refined mass balance results may be obtained at the expense of a finer time-stepping sequence.

The sample problems presented in this chapter were intended to illustrate the use and capabilities of FEMTRAN. The problems also serve as benchmark calculations when analytic or semi-analytic results were available. The problems presented here were for saturated media and uniform flow. Additional problems have been computed with FEMTRAN for transport by transient, saturated/unsaturated flow fields. These results are forthcoming[14].

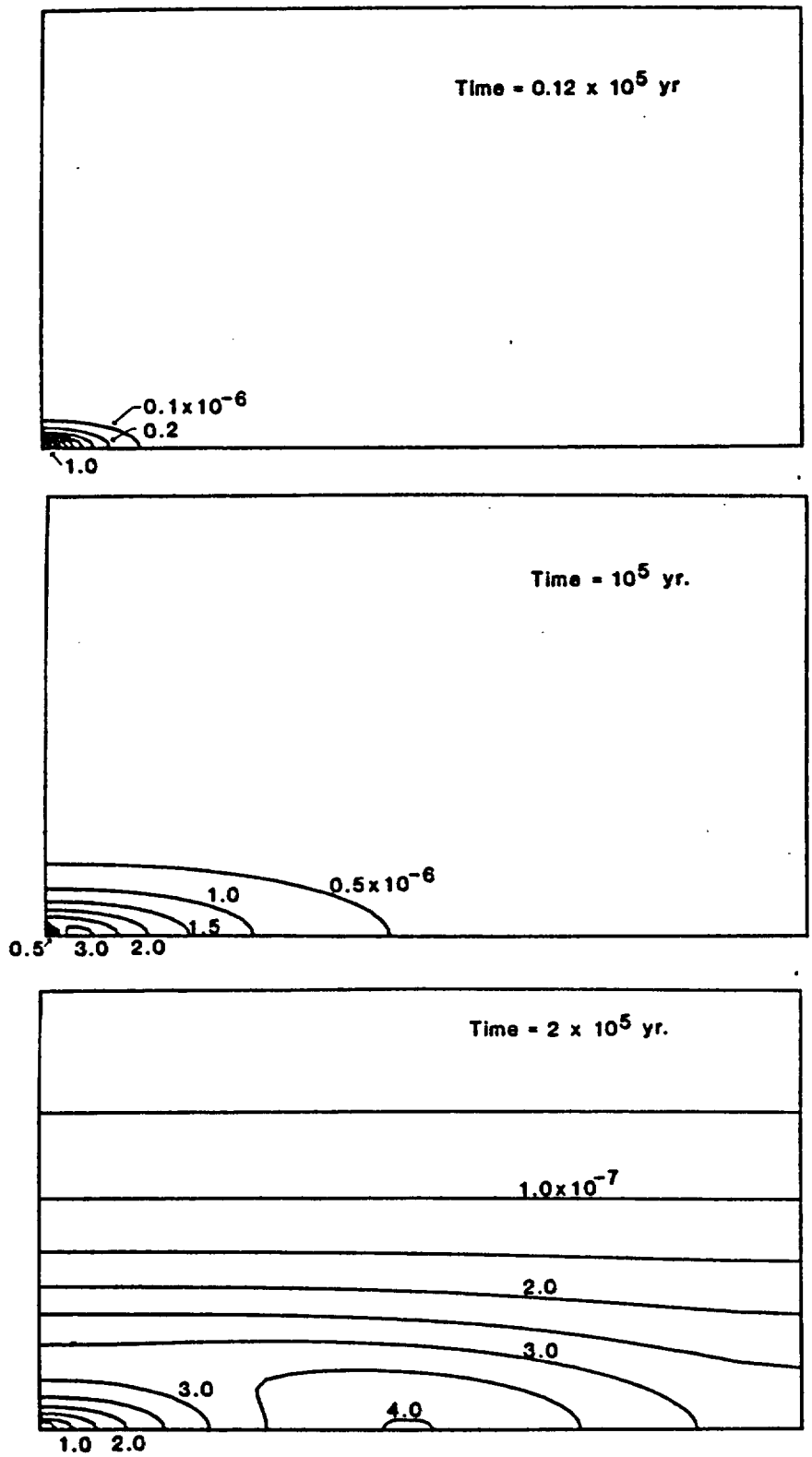

Figure 16. Contours of Activity for ^{230}Th -- Sample Problem 3

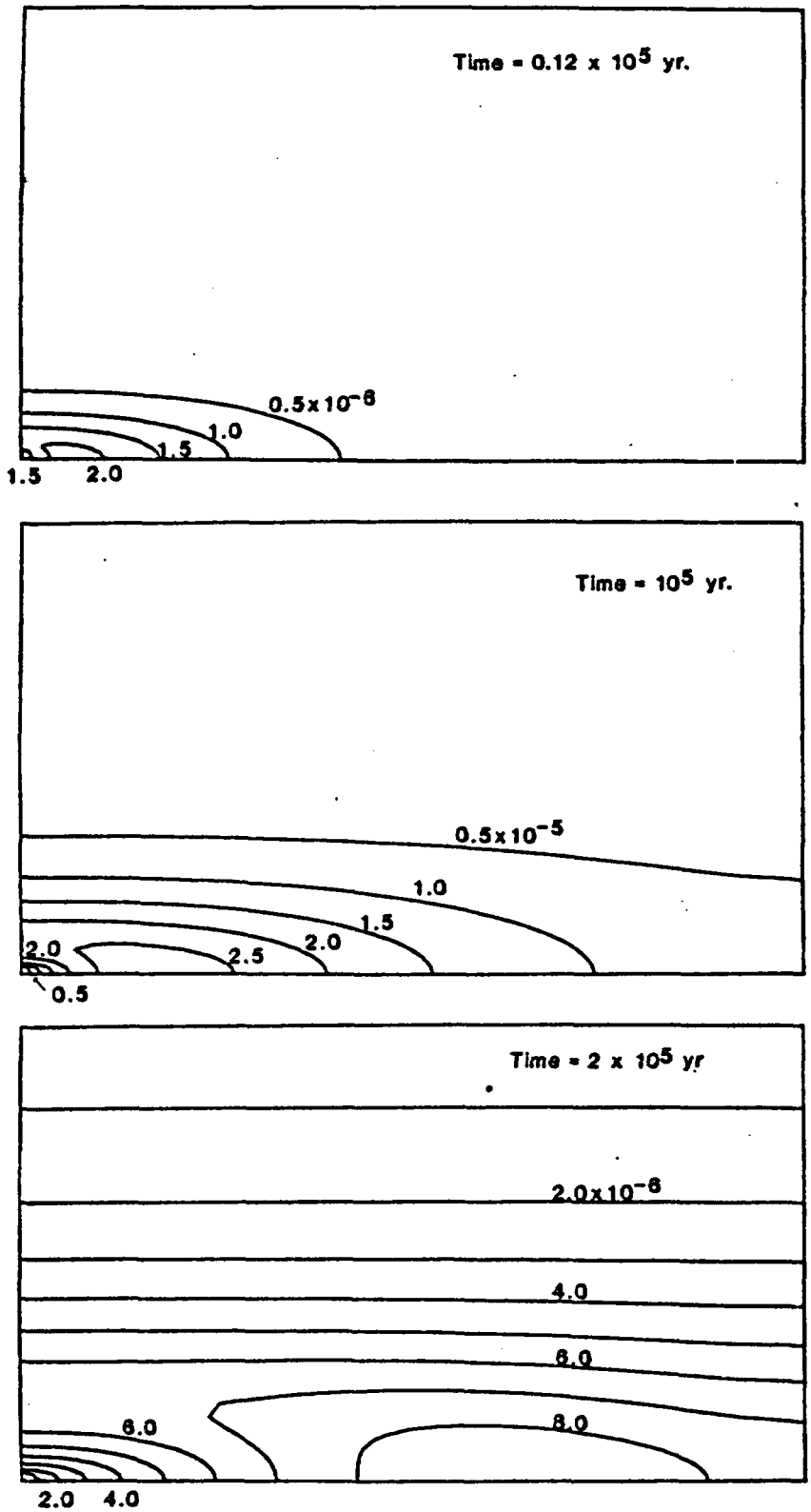

Figure 17. Contours of Activity for ^{226}Ra -- Sample Problem 3

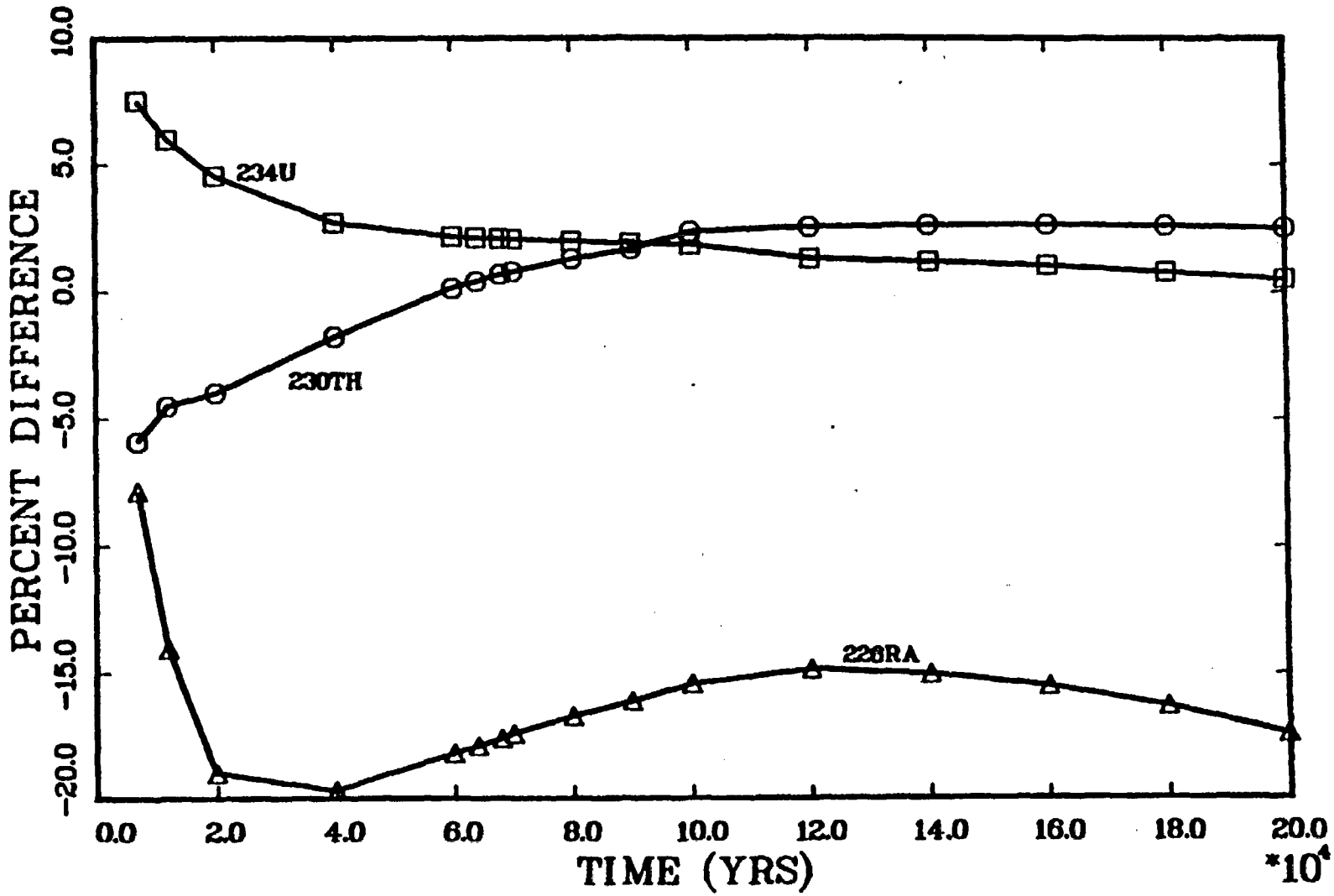

Figure 18. Cumulative Mass Balance History for Sample Problem 3

REFERENCES

1. J. O. Duguid, and M. Reeves, "Material Transport Through Porous Media: A Finite Element Galerkin Model," ORNL 4928, Environmental Sciences Div., ORNL, Oak Ridge, Tennessee, March 1976.
2. G. T. Yeh, and D. S. Ward, "FEMWASTE: A Finite Element Model of Waste Transport Through Saturated-Unsaturated Porous Media," ORNL 5601, Environmental Sciences Div., Oak Ridge National Laboratory, Oak Ridge, Tennessee, April 1981.
3. J. Bear, Dynamics of Fluids in Porous Media, 764 pp., Elsevier, New York, 1972.
4. H. Bateman, "The Solution of a System of Differential Equations Occurring in the Theory of Radioactive Transformations," Proc. Cambridge Phil. Soc. 15, pp. 423, 1910.
5. T. H. Pigford, et al., "Migration of Radionuclides Through Sorbing Media Analytical Solutions -- II," LBL-11616, Lawrence Berkeley Laboratory, Berkeley, California, October 1980.
6. K. H. Huebner, and Thornton, E. A., The Finite Element Method for Engineers, pp. 623, John Wiley and Sons, New York, 1982.
7. I. Ergatoudis, B. M. Irons, and D. C. Zienkiewicz, "Curved Isoparametric, Quadrilateral' Elements for Finite Element Analysis," Int. J. Solids Struct. 4, 1968.
8. L. Christie, et al., "Finite Element Methods for Second Order Differential Equations with Significant First derivatives," Int. J. Num. Meth. Engrg., 10, pp. 1389-1396, 1976.
9. J. C. Heinrich, et al., "An Upwind Finite Element Scheme for Two-Dimensional Convective Transport Equations," Int. J. Num. Meth. Engrg., 11, pp. 131-143, 1977.
10. P. S. Huyakorn and K. Nilkuha, "Solution of Transient Transport Equation Using an Upstream Finite Element Scheme," Appl. Math. Model, 3, IPC Business Press, February 1979.
11. C. Desai, and J. Abel., Introduction to the Finite Element Method: A Numerical Method for Engineering Analysis. Van Nostrand Reinhold, New York, 1972.

12. D. K. Gartling and C. E. Hickox, "MARIAH -- A Finite Element Computer Program for Incompressible Porous Flow Problems: Theoretical Background," SAND79-1622, Sandia National Laboratories, Albuquerque, NM, Sept. 1982.

13. R. R. Eaton, D. K. Gartling and D. E. Larson, "SAGUARO -- A Finite Element Computer Program for Partially Saturated Porous Flow Problems," SAND82-2772, Sandia National Laboratories, Albuquerque, NM, June 1983.

14. M. J. Martinez and R. R. Eaton, "COVE Benchmark Calculations with SAGUARO and FEMTRAN," Sandia National Laboratories, (in preparation).

15. G. T. Yeh and D. S. Ward, "FEMWATER: A Finite Element Model of Water Flow Through Saturated-Unsaturated Porous Media," ORNL 5567, Environmental Sciences Div., ORNL, Oak Ridge, Tennessee, October 1980.

16. R. E. Jones, "QMESH: A Self-Organizing Mesh Generation Program," SLA-73-1088, Sandia National Laboratories, National Technical Information Service.

17. M. J. Martinez and N. E. Bixler, "DECODE-A Direct Data Transfer Routine for Using SAGUARO Mesh and Solution Data in FEMTRAN," memo to Distribution, March 30, 1984.

18. D. K. Gartling, "MERLIN -- A Computer Program to Transfer Data Between Finite Element Meshes," SAND81-0463, Sandia National Laboratories, Albuquerque, NM, September 1981.

19. R. T. Dillon, R. B. Lantz and S. B. Pahwa, "Risk Methodology for Geologic Disposal of Radioactive Waste: The Sandia Waste Isolation Flow and Transport (SWIFT) Model," SAND78-1267, Sandia National Laboratories, Albuquerque, NM, October 1978.

20. P. Huyakorn and B. Lester, "FTRANS: Finite Elements Model for Simulating Fluid Flow and Transport of Radioactive Nuclides in Fractured Porous Media," INTERA Environmental Consultants, Inc., Report ONWI/sub/82/E512-02900/CD021, May 1982.

21. J. Haderman, "Working Paper for the INTRACOIN Study, Level 1," EIR-internal report TM-45-81-23 (2.6.81).

22. J. Haderman and J. Patry, Nucl. Technol., 54, pp. 226, (1981).

APPENDIX

(FEMTRAN Output for Sample Problem 1)

```
PROBLEM    1..  LESTER'S PROBLEM


INPUT TABLE 1.. BASIC PARAMETERS

     NUMBER OF NODAL POINTS. . . . . . . . .  156
     NUMBER OF ELEMENTS. . . . . . . . . . .   77
     NUMBER OF DIFFERENT MATERIALS . . . . .    1
     NUMBER OF CORRECTION MATERIALS. . . . .    0
     NUMBER OF TIME INCREMENTS . . . . . . .   42
     NUMBER OF BOUNDARY CONDITIONS . . . . .    0
     NUMBER OF SURFACE TERMS . . . . . . . .    3
     VELOCITY INPUT CONTROL. . . . . . . . .    1
     AUXILIARY STORAGE CONTROL . . . . . . .    1
     STEADY-STATE CONTROL. . . . . . . . . .    1
     NO. OF MATERIAL PROPERTY PER MATERIAL .    8
     UPSTREAM WEIGHTING INDICATOR, IWET. . .    0
     LUMPING INDICATOR, ILUMP. . . . . . . .    0
     TIME-DIFFERENCE INDICATOR, IMID . . . .    0
     NO. SPECIES IN CHAIN  . . . . . . . . .    3
     TRANSIENT BC CONTROL  . . . . . . . . .    1
     MESH AND NODE INPUT CONTROL . . . . . .    0
     HYDROLOGIC DATA INPUT CONTROL . . . . .    0
     CONTINUOUS FLOW FIELD CONTROL . . . . .    0
     HYDROLOGIC MASS BALANCE CONTROL . . . .    1

     TIME INCREMENT. . . . . . . . . . . . .0.9100E+01
     MULTIPLIER FOR INCREASING DELT. . . . .  0.000000
     MAXIMUM VALUE OF DELT . . . . . . . . .0.9100E+01
     MAXIMUM VALUE OF TIME . . . . . . . . .0.2739E+03
     TIME-INTEGRATION PARAMETER. . . . . . .  0.500000
     LEACH TIME FOR RADIONUCLIDES  . . . . .0.3000E+03


    SPECIE NO.,NBC(I),I=1,NSPEC
  0   0   0


    SPECIE NO.,NST(I),I=1,NSPEC
  1   1   1


    HEAD CONVERSION          FLUX CONVERSION
    0.1000E+01               0.1000E+01


     OUTPUT CONTROL
          3 1 0 0 0 2 0 1 0 0 2 0 1 0 0 1 0 1 0 0 2 0 1 0 0 1 0 1 0 2 2 0 0 0 0 0 0 0 0
          2 0 0



     AUXILIARY STORAGE AND FLOW FIELD PRINT CONTROL
          1 1 0 0 0 0 0 0 1 0 0 0 0 0 0 0 0 0 1 0 0 0 0 0 0 0 0 1 0 0 0 0 0 0 0 0 0 0
          1 0 0
```

INPUT TABLE 2.. MATERIAL PROPERTIES

MAT. NO.	KD	RHOB	AL	AT	LAMBDA	POR	ALP	AM
1	0.0000E+00	0.1000E+01	0.8500E+01	0.0000E+00	0.0000E+00	0.1000E+00	0.0000E+00	0.0000E+00

SPECIES DEPENDENT PROPERTIES

MAT. NO.	KD	LAMBDA	DIFF COEF
		SPECIE NO.	1
1	0.9351E+03	0.1600E-02	0.0000E+00
		SPECIE NO.	2
1	0.9351E+03	0.4620E-01	0.0000E+00
		SPECIE NO.	3
1	0.9351E+03	0.1060E-03	0.0000E+00

INPUT TABLE 3.. NODAL POINT DATA

NODE	X	Z	NODE	X	Z	NODE	X	Z
1	0.0000E+00	0.0000E+00	2	0.1000E+01	0.0000E+00	3	0.2000E+01	0.0000E+00
4	0.3000E+01	0.0000E+00	5	0.4000E+01	0.0000E+00	6	0.5000E+01	0.0000E+00
7	0.0000E+00	0.1000E+01	8	0.1000E+01	0.1000E+01	9	0.2000E+01	0.1000E+01
10	0.3000E+01	0.1000E+01	11	0.4000E+01	0.1000E+01	12	0.5000E+01	0.1000E+01
13	0.7500E+01	0.0000E+00	14	0.1000E+02	0.0000E+00	15	0.1250E+02	0.0000E+00
16	0.1500E+02	0.0000E+00	17	0.1750E+02	0.0000E+00	18	0.2000E+02	0.0000E+00
19	0.7500E+01	0.1000E+01	20	0.1000E+02	0.1000E+01	21	0.1250E+02	0.1000E+01
22	0.1500E+02	0.1000E+01	23	0.1750E+02	0.1000E+01	24	0.2000E+02	0.1000E+01
25	0.2500E+02	0.0000E+00	26	0.3000E+02	0.0000E+00	27	0.3500E+02	0.0000E+00
28	0.4000E+02	0.0000E+00	29	0.4500E+02	0.0000E+00	30	0.2500E+02	0.1000E+01
31	0.3000E+02	0.1000E+01	32	0.3500E+02	0.1000E+01	33	0.4000E+02	0.1000E+01
34	0.4500E+02	0.1000E+01	35	0.5000E+02	0.1000E+01	36	0.5500E+02	0.1000E+01
37	0.6000E+02	0.1000E+01	38	0.6500E+02	0.1000E+01	39	0.7000E+02	0.1000E+01
40	0.5000E+02	0.0000E+00	41	0.5500E+02	0.0000E+00	42	0.6000E+02	0.0000E+00
43	0.6500E+02	0.0000E+00	44	0.7000E+02	0.0000E+00	45	0.7500E+02	0.0000E+00
46	0.8000E+02	0.0000E+00	47	0.8500E+02	0.0000E+00	48	0.9000E+02	0.0000E+00
49	0.9500E+02	0.0000E+00	50	0.7500E+02	0.1000E+01	51	0.8000E+02	0.1000E+01
52	0.8500E+02	0.1000E+01	53	0.9000E+02	0.1000E+01	54	0.9500E+02	0.1000E+01
55	0.1000E+03	0.1000E+01	56	0.1000E+03	0.0000E+00	57	0.1100E+03	0.0000E+00
58	0.1200E+03	0.0000E+00	59	0.1300E+03	0.0000E+00	60	0.1400E+03	0.0000E+00
61	0.1500E+03	0.0000E+00	62	0.1100E+03	0.1000E+01	63	0.1200E+03	0.1000E+01
64	0.1300E+03	0.1000E+01	65	0.1400E+03	0.1000E+01	66	0.1500E+03	0.1000E+01
67	0.1600E+03	0.1000E+01	68	0.1700E+03	0.1000E+01	69	0.1800E+03	0.1000E+01
70	0.1900E+03	0.1000E+01	71	0.2000E+03	0.1000E+01	72	0.1600E+03	0.0000E+00
73	0.1700E+03	0.0000E+00	74	0.1800E+03	0.0000E+00	75	0.1900E+03	0.0000E+00
76	0.2000E+03	0.0000E+00	77	0.2100E+03	0.0000E+00	78	0.2200E+03	0.0000E+00
79	0.2300E+03	0.0000E+00	80	0.2400E+03	0.0000E+00	81	0.2500E+03	0.0000E+00
82	0.2100E+03	0.1000E+01	83	0.2200E+03	0.1000E+01	84	0.2300E+03	0.1000E+01
85	0.2400E+03	0.1000E+01	86	0.2500E+03	0.1000E+01	87	0.2600E+03	0.1000E+01
88	0.2700E+03	0.1000E+01	89	0.2800E+03	0.1000E+01	90	0.2900E+03	0.1000E+01
91	0.3000E+03	0.1000E+01	92	0.2600E+03	0.0000E+00	93	0.2700E+03	0.0000E+00
94	0.2800E+03	0.0000E+00	95	0.2900E+03	0.0000E+00	96	0.3000E+03	0.0000E+00
97	0.3100E+03	0.0000E+00	98	0.3200E+03	0.0000E+00	99	0.3300E+03	0.0000E+00
100	0.3400E+03	0.0000E+00	101	0.3500E+03	0.0000E+00	102	0.3100E+03	0.1000E+01
103	0.3200E+03	0.1000E+01	104	0.3300E+03	0.1000E+01	105	0.3400E+03	0.1000E+01
106	0.3500E+03	0.1000E+01	107	0.3600E+03	0.1000E+01	108	0.3700E+03	0.1000E+01
109	0.3800E+03	0.1000E+01	110	0.3900E+03	0.1000E+01	111	0.4000E+03	0.1000E+01
112	0.3600E+03	0.0000E+00	113	0.3700E+03	0.0000E+00	114	0.3800E+03	0.0000E+00
115	0.3900E+03	0.0000E+00	116	0.4000E+03	0.0000E+00	117	0.4100E+03	0.0000E+00
118	0.4200E+03	0.0000E+00	119	0.4300E+03	0.0000E+00	120	0.4400E+03	0.0000E+00
121	0.4500E+03	0.0000E+00	122	0.4100E+03	0.1000E+01	123	0.4200E+03	0.1000E+01
124	0.4300E+03	0.1000E+01	125	0.4400E+03	0.1000E+01	126	0.4500E+03	0.1000E+01
127	0.4600E+03	0.1000E+01	128	0.4700E+03	0.1000E+01	129	0.4800E+03	0.1000E+01
130	0.4900E+03	0.1000E+01	131	0.5000E+03	0.1000E+01	132	0.4600E+03	0.0000E+00
133	0.4700E+03	0.0000E+00	134	0.4800E+03	0.0000E+00	135	0.4900E+03	0.0000E+00
136	0.5000E+03	0.0000E+00	137	0.5500E+03	0.0000E+00	138	0.6000E+03	0.0000E+00
139	0.6500E+03	0.0000E+00	140	0.7000E+03	0.0000E+00	141	0.7500E+03	0.0000E+00
142	0.5500E+03	0.1000E+01	143	0.6000E+03	0.1000E+01	144	0.6500E+03	0.1000E+01
145	0.7000E+03	0.1000E+01	146	0.7500E+03	0.1000E+01	147	0.8000E+03	0.1000E+01
148	0.8500E+03	0.1000E+01	149	0.9000E+03	0.1000E+01	150	0.9500E+03	0.1000E+01

INPUT TABLE 3.. NODAL POINT DATA

NODE	X	Z	NODE	X	Z	NODE	X	Z
151	0.1000E+04	0.1000E+01	152	0.8000E+03	0.0000E+00	153	0.8500E+03	0.0000E+00
154	0.9000E+03	0.0000E+00	155	0.9500E+03	0.0000E+00	156	0.1000E+04	0.0000E+00

INPUT TABLE 4.. ELEMENT DATA

	GLOBAL INDICES OF ELEMENT NODES					
ELEMENT	1	2	3	4	MATERIAL	NODE DIFF.
1	1	2	8	7	1	7
2	2	3	9	8	1	7
3	3	4	10	9	1	7
4	4	5	11	10	1	7
5	5	6	12	11	1	7
6	6	13	19	12	1	13
7	13	14	20	19	1	7
8	14	15	21	20	1	7
9	15	16	22	21	1	7
10	16	17	23	22	1	7
11	17	18	24	23	1	7
12	18	25	30	24	1	12
13	25	26	31	30	1	6
14	26	27	32	31	1	6
15	27	28	33	32	1	6
16	28	29	34	33	1	6
17	29	40	35	34	1	11
18	40	41	36	35	1	6
19	41	42	37	36	1	6
20	42	43	38	37	1	6
21	43	44	39	38	1	6
22	44	45	50	39	1	11
23	45	46	51	50	1	6
24	46	47	52	51	1	6
25	47	48	53	52	1	6
26	48	49	54	53	1	6
27	49	56	55	54	1	7
28	56	57	62	55	1	7
29	57	58	63	62	1	6
30	58	59	64	63	1	6
31	59	60	65	64	1	6
32	60	61	66	65	1	6
33	61	72	67	66	1	11
34	72	73	68	67	1	6
35	73	74	69	68	1	6
36	74	75	70	69	1	6
37	75	76	71	70	1	6
38	76	77	82	71	1	11
39	77	78	83	82	1	6
40	78	79	84	83	1	6
41	79	80	85	84	1	6
42	80	81	86	85	1	6
43	81	92	87	86	1	11
44	92	93	88	87	1	6
45	93	94	89	88	1	6
46	94	95	90	89	1	6
47	95	96	91	90	1	6
48	96	97	102	91	1	11
49	97	98	103	102	1	6
50	98	99	104	103	1	6

ELEMENT	GLOBAL INDICES OF ELEMENT NODES 1	2	3	4	MATERIAL	NODE DIFF.
51	99	100	105	104	1	6
52	100	101	106	105	1	6
53	101	112	107	106	1	11
54	112	113	108	107	1	6
55	113	114	109	108	1	6
56	114	115	110	109	1	6
57	115	116	111	110	1	6
58	116	117	122	111	1	11
59	117	118	123	122	1	6
60	118	119	124	123	1	6
61	119	120	125	124	1	6
62	120	121	126	125	1	6
63	121	132	127	126	1	11
64	132	133	128	127	1	6
65	133	134	129	128	1	6
66	134	135	130	129	1	6
67	135	136	131	130	1	6
68	136	137	142	131	1	11
69	137	138	143	142	1	6
70	138	139	144	143	1	6
71	139	140	145	144	1	6
72	140	141	146	145	1	6
73	141	152	147	146	1	11
74	152	153	148	147	1	6
75	153	154	149	148	1	6
76	154	155	150	149	1	6
77	155	156	151	150	1	6

INPUT TABLE 5 TRANSIENT B. C. PARAMETERS

NO. OF DIRICHLET B. C. NODES 0
NO. OF CAUCHY B. C. ELEMENT-SIDES, NST 3

INPUT TABLE 6 FOR SPECIE 1 TRANSIENT STATE CAUCHY B. C. AT ELEMENT MI E=EI AT NODE NI, E=EJ AT NODE NJ

MI	NI	NJ	EI	EJ		
1	1	7	2.3940E+02	2.3940E+02	1.0000E+00	1.0000E+00

INPUT TABLE 6 FOR SPECIE 2 TRANSIENT STATE CAUCHY B. C. AT ELEMENT MI E=EI AT NODE NI, E=EJ AT NODE NJ

MI	NI	NJ	EI	EJ		
1	1	7	0.0000E+00	0.0000E+00	0.0000E+00	0.0000E+00

INPUT TABLE 6 FOR SPECIE 3 TRANSIENT STATE CAUCHY B. C. AT ELEMENT MI E=EI AT NODE NI, E=EJ AT NODE NJ

MI	NI	NJ	EI	EJ		
1	1	7	0.0000E+00	0.0000E+00	0.0000E+00	0.0000E+00

****

SYSTEM-FLOW TABLE 37.. AT TIME = 2.7300E+02 ,(DELT = 9.1000E+00) ITIM= 30 SPECIE NO.= 1

TYPE OF FLOW	RATE	INC. FLOW	TOTAL FLOW
DIRICHLET NODE FLOW	0.0000E+00	0.0000E+00	0.0000E+00
CAUCHY FLUX-NODE FLOW	-0.1542E+03	-0.1408E+04	-0.5152E+05
SEEPAGE FLUX-NODE FLOW.	0.0000E+00	0.0000E+00	0.0000E+00
NEUMANN FLUX NODE FLOW.	-0.3911E-10	-0.3565E-09	-0.6577E-08
NET FLOW.	-0.1542E+03	-0.1408E+04	-0.5152E+05
INCREASE IN MATERIAL CONTENT (LIQUID) .	0.9443E-02	0.8593E-01	0.4478E+01
INCREASE IN MATERIAL CONTENT (SOLID). .	0.8830E+02	0.8035E+03	0.4188E+05
RADIOACTIVE LOSSES (LIQUID AND SOLID) .	0.6637E+02	0.6040E+03	0.1063E+05
INCREASE DUE TO COMP. OF SKELTON . . .	0.0000E+00	0.0000E+00	0.0000E+00
NET ACCUMULATION	0.1547E+03	0.1408E+04	0.5251E+05
PERCENT MASS BALANCE ERROR	-0.3085E+00	0.1970E-01	-0.1878E+01

OUTPUT TABLE 19.. CONCENTRATIONS AT TIME = 2.7300E+02 ,(DELT = 9.1000E+00),(BAND WIDTH = 27)

*** ITIME = 30 SPECIE NO. = 1

NODE I	CONCENTRATION AT NODES I,I+1,...,I+7							
1	6.3463E-01	6.3358E-01	6.3275E-01	6.3179E-01	6.3074E-01	6.2962E-01	6.3463E-01	6.3358E-01
9	6.3275E-01	6.3179E-01	6.3074E-01	6.2962E-01	6.2848E-01	6.2282E-01	6.1857E-01	6.1370E-01
17	6.0816E-01	6.0189E-01	6.2648E-01	6.2282E-01	6.1857E-01	6.1370E-01	6.0816E-01	6.0189E-01
25	5.8690E-01	5.6853E-01	5.4660E-01	5.2111E-01	4.9218E-01	5.8690E-01	5.6853E-01	5.4660E-01
33	5.2111E-01	4.9218E-01	4.6014E-01	4.2546E-01	3.8877E-01	3.5082E-01	3.1244E-01	4.6014E-01
41	4.2546E-01	3.8877E-01	3.5082E-01	3.1244E-01	2.7445E-01	2.3765E-01	2.0275E-01	1.7031E-01
49	1.4074E-01	2.7445E-01	2.3765E-01	2.0275E-01	1.7031E-01	1.4074E-01	1.1425E-01	1.1425E-01
57	7.2125E-02	4.2595E-02	2.3491E-02	1.2081E-02	5.7868E-03	7.2125E-02	4.2595E-02	2.3491E-02
65	1.2081E-02	5.7868E-03	2.5797E-03	1.0697E-03	4.1243E-04	1.4789E-04	4.9349E-05	2.5797E-03
73	1.0697E-03	4.1243E-04	1.4789E-04	4.9349E-05	1.5340E-05	4.4492E-06	1.2069E-06	3.0713E-07
81	7.3590E-08	1.5340E-05	4.4492E-06	1.2069E-06	3.0713E-07	7.3590E-08	1.6675E-08	3.5907E-09
89	7.3857E-10	1.4587E-10	2.7800E-11	1.6675E-08	3.5907E-09	7.3857E-10	1.4587E-10	2.7800E-11
97	5.1367E-12	9.2394E-13	1.6236E-13	2.7957E-14	4.7295E-15	5.1367E-12	9.2394E-13	1.6236E-13
105	2.7957E-14	4.7295E-15	7.8771E-16	1.2941E-16	2.1001E-17	3.3713E-18	5.3595E-19	7.8771E-16
113	1.2941E-16	2.1001E-17	3.3713E-18	5.3595E-19	8.4453E-20	1.3202E-20	2.0490E-21	3.1592E-22
121	4.8415E-23	8.4453E-20	1.3202E-20	2.0490E-21	3.1592E-22	4.8415E-23	7.3784E-24	1.1187E-24
129	1.6881E-25	2.5496E-26	2.0265E-27	7.3784E-24	1.1187E-24	1.6881E-25	2.5496E-26	2.0265E-27
137	-4.2067E-28	8.7318E-29	-1.8123E-29	3.7609E-30	-7.8040E-31	-4.2067E-28	8.7318E-29	-1.8123E-29
145	3.7609E-30	-7.8040E-31	1.6192E-31	-3.3597E-32	6.9886E-33	-1.5175E-33	5.5473E-34	1.6192E-31
153	-3.3597E-32	6.9886E-33	-1.5175E-33	5.5473E-34				

****

SYSTEM-FLOW TABLE 38., AT TIME = 2.7300E+02 ,(DELT = 9.1000E+00) ITIM= 30 SPECIE NO.= 2

TYPE OF FLOW	RATE	INC. FLOW	TOTAL FLOW
DIRICHLET NODE FLOW	0.0000E+00	0.0000E+00	0.0000E+00
CAUCHY FLUX-NODE FLOW	-0.5410E+01	-0.5051E+02	-0.1708E+04
SEEPAGE FLUX-NODE FLOW.	0.0000E+00	0.0000E+00	0.0000E+00
NEUMANN FLUX NODE FLOW.	-0.1421E-11	-0.1296E-10	-0.2381E-09
NET FLOW.	-0.5410E+01	-0.5051E+02	-0.1708E+04
INCREASE IN MATERIAL CONTENT (LIQUID) .	0.3318E-03	0.3020E-02	0.1623E+00
INCREASE IN MATERIAL CONTENT (SOLID). .	0.3103E+01	0.2824E+02	0.1517E+04
RADIOACTIVE LOSSES (LIQUID AND SOLID) .	0.3088E+01	0.2810E+02	0.4721E+03
INCREASE DUE TO COMP. OF SKELTON . . .	0.0000E+00	0.0000E+00	0.0000E+00
NET ACCUMULATION	0.6192E+01	0.5635E+02	0.1990E+04
PERCENT MASS BALANCE ERROR	-0.1262E+02	-0.1035E+02	-0.1416E+02

OUTPUT TABLE 20., CONCENTRATIONS AT TIME = 2.7300E+02 ,(DELT = 9.1000E+00),(BAND WIDTH = 27)

*** ITIME = 30 SPECIE NO. = 2

NODE I	CONCENTRATION AT NODES I,I+1,...,I+7							
1	2.2680E-02	2.2676E-02	2.2626E-02	2.2584E-02	2.2544E-02	2.2501E-02	2.2680E-02	2.2676E-02
9	2.2626E-02	2.2584E-02	2.2544E-02	2.2501E-02	2.2382E-02	2.2249E-02	2.2097E-02	2.1926E-02
17	2.1733E-02	2.1516E-02	2.2382E-02	2.2249E-02	2.2097E-02	2.1926E-02	2.1733E-02	2.1516E-02
25	2.1000E-02	2.0370E-02	1.9616E-02	1.8739E-02	1.7740E-02	2.1000E-02	2.0370E-02	1.9616E-02
33	1.8739E-02	1.7740E-02	1.6629E-02	1.5423E-02	1.4140E-02	1.2808E-02	1.1453E-02	1.6629E-02
41	1.5423E-02	1.4140E-02	1.2808E-02	1.1453E-02	1.0105E-02	8.7913E-03	7.5379E-03	6.3659E-03
49	5.2908E-03	1.0105E-02	8.7913E-03	7.5379E-03	6.3659E-03	5.2908E-03	4.3214E-03	4.3214E-03
57	2.7628E-03	1.6541E-03	9.2561E-04	4.8340E-04	2.3531E-04	2.7628E-03	1.6541E-03	9.2561E-04
65	4.8340E-04	2.3531E-04	1.0666E-04	4.4990E-05	1.7651E-05	6.4410E-06	2.1869E-06	1.0666E-04
73	4.4990E-05	1.7651E-05	6.4410E-06	2.1869E-06	6.9145E-07	2.0389E-07	5.6188E-08	1.4511E-08
81	3.5249E-09	6.9145E-07	2.0389E-07	5.6188E-08	1.4511E-08	3.5249E-09	8.0867E-10	1.7607E-10
89	3.6567E-11	7.2828E-12	1.3981E-12	8.0867E-10	1.7607E-10	3.6567E-11	7.2828E-12	1.3981E-12
97	2.5993E-13	4.7002E-14	8.2972E-15	1.4344E-15	2.4348E-16	2.5993E-13	4.7002E-14	8.2972E-15
105	1.4344E-15	2.4348E-16	4.0675E-17	6.6999E-18	1.0899E-18	1.7532E-19	2.7923E-20	4.0675E-17
113	6.6999E-18	1.0899E-18	1.7532E-19	2.7923E-20	4.4075E-21	6.9007E-22	1.0725E-22	1.6556E-23
121	2.5401E-24	4.4075E-21	6.9007E-22	1.0725E-22	1.6556E-23	2.5401E-24	3.8753E-25	5.8815E-26
129	8.8830E-27	1.3427E-27	1.0682E-28	3.8753E-25	5.8815E-26	8.8830E-27	1.3427E-27	1.0682E-28
137	-2.2172E-29	4.6015E-30	-9.5492E-31	1.9814E-31	-4.1110E-32	-2.2172E-29	4.6015E-30	-9.5492E-31
145	1.9814E-31	-4.1110E-32	8.5286E-33	-1.7694E-33	3.6800E-34	-7.9898E-35	2.9202E-35	8.5286E-33
153	-1.7694E-33	3.6800E-34	-7.9898E-35	2.9202E-35				

****

SYSTEM-FLOW TABLE 39.. AT TIME = 2.7300E+02 ,(DELT = 9.1000E+00) ITIM= 30 SPECIE NO.= 3

TYPE OF FLOW	RATE	INC. FLOW	TOTAL FLOW
DIRICHLET NODE FLOW	0.0000E+00	0.0000E+00	0.0000E+00
CAUCHY FLUX-NODE FLOW	-0.7867E+02	-0.7105E+03	-0.1092E+05
SEEPAGE FLUX-NODE FLOW.	0.0000E+00	0.0000E+00	0.0000E+00
NEUMANN FLUX NODE FLOW.	-0.2046E-10	-0.1819E-09	-0.2003E-08
NET FLOW.	-0.7867E+02	-0.7105E+03	-0.1092E+05
INCREASE IN MATERIAL CONTENT (LIQUID) .	0.1560E-01	0.1420E+00	0.2368E+01
INCREASE IN MATERIAL CONTENT (SOLID). .	0.1459E+03	0.1327E+04	0.2214E+05
RADIOACTIVE LOSSES (LIQUID AND SOLID) .	-0.6718E+02	-0.6113E+03	-0.1088E+05
INCREASE DUE TO COMP. OF SKELTON . . .	0.0000E+00	0.0000E+00	0.0000E+00
NET ACCUMULATION	0.7870E+02	0.7162E+03	0.1127E+05
PERCENT MASS BALANCE ERROR	-0.3774E-01	-0.7973E+00	-0.3043E+01

OUTPUT TABLE 21.. CONCENTRATIONS AT TIME = 2.7300E+02 ,(DELT = 9.1000E+00),(BAND WIDTH = 27)

*** ITIME = 30 SPECIE NO. = 3

NODE I	CONCENTRATION AT NODES I,I+1,...,I+7							
1	3.2699E-01	3.2673E-01	3.2619E-01	3.2567E-01	3.2514E-01	3.2457E-01	3.2699E-01	3.2673E-01
9	3.2619E-01	3.2567E-01	3.2514E-01	3.2457E-01	3.2297E-01	3.2113E-01	3.1901E-01	3.1659E-01
17	3.1386E-01	3.1078E-01	3.2297E-01	3.2113E-01	3.1901E-01	3.1659E-01	3.1386E-01	3.1078E-01
25	3.0346E-01	2.9453E-01	2.8388E-01	2.7148E-01	2.5738E-01	3.0346E-01	2.9453E-01	2.8388E-01
33	2.7148E-01	2.5738E-01	2.4170E-01	2.2464E-01	2.0649E-01	1.8758E-01	1.6830E-01	2.4170E-01
41	2.2464E-01	2.0649E-01	1.8758E-01	1.6830E-01	1.4904E-01	1.3021E-01	1.1216E-01	9.5207E-02
49	7.9570E-02	1.4904E-01	1.3021E-01	1.1216E-01	9.5207E-02	7.9570E-02	6.5394E-02	6.5394E-02
57	4.2373E-02	2.5762E-02	1.4670E-02	7.8138E-03	3.8882E-03	4.2373E-02	2.5762E-02	1.4670E-02
65	7.8138E-03	3.8882E-03	1.8059E-03	7.8238E-04	3.1607E-04	1.1905E-04	4.1825E-05	1.8059E-03
73	7.8238E-04	3.1607E-04	1.1905E-04	4.1825E-05	1.3715E-05	4.2028E-06	1.2058E-06	3.2466E-07
81	8.2296E-08	1.3715E-05	4.2028E-06	1.2058E-06	3.2466E-07	8.2296E-08	1.9711E-08	4.4800E-09
89	9.7079E-10	2.0154E-10	4.0282E-11	1.9711E-08	4.4800E-09	9.7079E-10	2.0154E-10	4.0282E-11
97	7.7872E-12	1.4623E-12	2.6772E-13	4.7947E-14	8.4234E-15	7.7872E-12	1.4623E-12	2.6772E-13
105	4.7947E-14	8.4234E-15	1.4551E-15	2.4763E-16	4.1591E-17	6.9039E-18	1.1340E-18	1.4551E-15
113	2.4763E-16	4.1591E-17	6.9039E-18	1.1340E-18	1.8452E-19	2.9769E-20	4.7654E-21	7.5749E-22
121	1.1963E-22	1.8452E-19	2.9769E-20	4.7654E-21	7.5749E-22	1.1963E-22	1.8782E-23	2.9327E-24
129	4.5560E-25	7.0821E-26	5.8173E-27	1.8782E-23	2.9327E-24	4.5560E-25	7.0821E-26	5.8173E-27
137	-1.2016E-27	2.4819E-28	-5.1254E-29	1.0583E-29	-2.1851E-30	-1.2016E-27	2.4819E-28	-5.1254E-29
145	1.0583E-29	-2.1851E-30	4.5109E-31	-9.3126E-32	1.9273E-32	-4.1624E-33	1.5124E-33	4.5109E-31
153	-9.3126E-32	1.9273E-32	-4.1624E-33	1.5124E-33				

DISTRIBUTION LIST

B. C. Rusche (RW-1)
Director
Office of Civilian Radioactive
Waste Management
U.S. Department of Energy
Forrestal Building
Washington, DC 20585

J. W. Bennett (RW-22)
Office of Geologic Repositories
U.S. Department of Energy
Forrestal Building
Washington, DC 20585

Ralph Stein (RW-23)
Office of Geologic Repositories
U.S. Department of Energy
Forrestal Building
Washington, DC 20585

J. J. Fiore, (RW-22)
Program Management Division
Office of Geologic Repositories
U.S. Department of Energy
Forrestal Building
Washington, DC 20585

M. W. Frei (RW-23)
Engineering & Licensing Division
Office of Geologic Repositories
U.S. Department of Energy
Forrestal Building
Washington, DC 20585

E. S. Burton (RW-25)
Siting Division
Office of Geologic Repositories
U.S. Department of Energy
Forrestal Building
Washington, D.C. 20585

C. R. Cooley (RW-24)
Geosciences & Technology Division
Office of Geologic Repositories
U.S. Department of Energy
Forrestal Building
Washington, DC 20585

T. P. Longo (RW-25)
Program Management Division
Office of Geologic Repositories
U.S. Department of Energy
Forrestal Building
Washington, DC 20585

Cy Klingsberg (RW-24)
Geosciences and Technology Division
Office of Geologic Repositories
U. S. Department of Energy
Forrestal Building
Washington, DC 20585

B. G. Gale (RW-25)
Siting Division
Office of Geologic Repositories
U.S. Department of Energy
Forrestal Building
Washington, D.C. 20585

R. J. Blaney (RW-22)
Program Management Division
Office of Geologic Repositories
U.S. Department of Energy
Forrestal Building
Washington, DC 20585

R. W. Gale (RW-40)
Office of Policy, Integration, and
Outreach
U.S. Department of Energy
Forrestal Building
Washington, D.C. 20585

J. E. Shaheen (RW-44)
Outreach Programs
Office of Policy, Integration and
Outreach
U.S. Department of Energy
Forrestal Building
Washington, DC 20585

J. O. Neff
Salt Repository Project Office
U.S. Department of Energy
505 King Avenue
Columbus, OH 43201

D. C. Newton (RW-23)
Engineering & Licensing Division
Office of Geologic Repositories
U.S. Department of Energy
Forrestal Building
Washington, DC 20585

O. L. Olson, Manager
Basalt Waste Isolation Project Office
U.S. Department of Energy
Richland Operations Office
Post Office Box 550
Richland, WA 99352

D. L. Vieth, Director (4)
Waste Management Project Office
U.S. Department of Energy
Post Office Box 14100
Las Vegas, NV 89114

D. F. Miller, Director
Office of Public Affairs
U.S. Department of Energy
Post Office Box 14100
Las Vegas, NV 89114

D. A. Nowack (14)
Office of Public Affairs
U.S. Department of Energy
Post Office Box 14100
Las Vegas, NV 89114

B. W. Church, Director
Health Physics Division
U.S. Department of Energy
Post Office Box 14100
Las Vegas, NV 89114

Chief, Repository Projects Branch
Division of Waste Management
U.S. Nuclear Regulatory Commission
Washington, D.C. 20555

S. A. Mann, Manager
Crystalline Rock Project Office
U.S. Department of Energy
9800 South Cass Avenue
Argonne, IL 60439

K. Street, Jr.
Lawrence Livermore National
Laboratory
Post Office Box 808
Mail Stop L-209
Livermore, CA 94550

L. D. Ramspott (3)
Technical Project Officer for NNWSI
Lawrence Livermore National
Laboratory
P.O. Box 808
Mail Stop L-204
Livermore, CA 94550

W. J. Purcell (RW-20)
Office of Geologic Repositories
U.S. Department of Energy
Forrestal Building
Washington, DC 20585

D. T. Oakley (3)
Technical Project Officer for NNWSI
Los Alamos National Laboratory
P.O. Box 1663
Mail Stop F-671
Los Alamos, NM 87545

W. W. Dudley, Jr. (4)
Technical Project Officer for NNWSI
U.S. Geological Survey
Post Office Box 25046
418 Federal Center
Denver, CO 80225

NTS Section Leader
Repository Project Branch
Division of Waste Management
U.S. Nuclear Regulatory Commission
Washington, D.C. 20555

Document Control Center
Division of Waste Management
U.S. Nuclear Regulatory Commission
Washington, D.C. 20555

P. T. Prestholt
NRC Site Representative
1050 East Flamingo Road
Suite 319
Las Vegas, NV 89109

M. E. Spaeth
Technical Project Officer for NNWSI
Science Applications
International, Corp.
2769 South Highland Drive
Las Vegas, NV 89109

SAIC-T&MSS Library (2)
Science Applications
International, Corp.
2950 South Highland Drive
Las Vegas, NV 89109

W. S. Twenhofel, Consultant
Science Applications
International, Corp.
820 Estes Street
Lakewood, CO 80215

A. E. Gurrola
General Manager
Energy Support Division
Holmes & Narver, Inc.
Post Office Box 14340
Las Vegas, NV 89114

J. A. Cross, Manager
Las Vegas Branch
Fenix & Scisson, Inc.
Post Office Box 15408
Las Vegas, NV 89114

N. E. Carter
Battelle Columbus Laboratory
Office of Nuclear Waste Isolation
505 King Avenue
Columbus, OH 43201

V. M. Glanzman
U.S. Geological Survey
Post Office Box 25046
913 Federal Center
Denver, CO 80225

J. B. Wright
Technical Project Officer for NNWSI
Westinghouse Electric Corporation
Waste Technology Services Division
Nevada Operations
Post Office Box 708
Mail Stop 703
Mercury, NV 89023

ONWI Library (2)
Battelle Columbus Laboratory
Office of Nuclear Waste Isolation
505 King Avenue
Columbus, OH 43201

W. M. Hewitt, Program Manager
Roy F. Weston, Inc.
2301 Research Blvd., 3rd Floor
Rockville, MD 20850

H. D. Cunningham
General Manager
Reynolds Electrical &
Engineering Co., Inc.
Post Office Box 14400
Mail Stop 555
Las Vegas, NV 89114

T. Hay, Executive Assistant
Office of the Governor
State of Nevada
Capitol Complex
Carson City, NV 89710

R. R. Loux, Jr., Director (8)
Nuclear Waste Project Office
State of Nevada
Capitol Complex
Carson City, NV 89710

C. H. Johnson, Technical
Program Manager
Nuclear Waste Project Office
State of Nevada
Capitol Complex
Carson City, NV 89710

John Fordham
Desert Research Institute
Water Resources Center
Post Office Box 60220
Reno, NV 89506

Dr. Martin Hifflin
Desert Research Institute
Water Resources Center
Suite 201
1500 East Tropicana Avenue
Las Vegas, NV 89109

Department of Comprehensive Planning
Clark County
225 Bridger Avenue, 7th Floor
Las Vegas, NV 89155

Planning Department
Nye County
Post Office Box 153
Tonopah, NV 89049

Lincoln County Commission
Lincoln County
Post Office Box 90
Pioche, NV 89043

Economic Development Department
City of Las Vegas
400 East Stewart Avenue
Las Vegas, NV 89101

Community Planning and Development
City of North Las Vegas
Post Office Box 4086
North Las Vegas, NV 89030

Internal Distribution:

1510 J. W. Nunziato
1511 G. G. Weigand
1511 N. E. Bixler
1511 R. R. Eaton
1511 D. K. Gartling
1511 M. J. Martinez (10)
1512 J. C. Cummings
1512 A. J. Russo
1513 D. W. Larson
1520 D. J. McCloskey
1530 L. W. Davison
1540 W. C. Luth
6300 R. W. Lynch
6310 T. O. Hunter
6311 L. W. Scully
6311 L. Perrine (2)
6312 F. W. Bingham
6312 A. L. Dudley
6312 J. Gauthier
6312 N. Hayden
6312 B. S. Langkopf
6312 Y. T. Lin
6312 S. Sinnock
6312 R. R. Peters
6313 J. R. Tillerson
6313 J. A. Fernandez
6313 E. A. Klavetter
6313 F. B. Nimick
6330 NNWSICF
6331 A. R. Lappin
6332 L. D. Tyler
6332 WMP Library
6334 D. R. Anderson
6334 J. Lipkin
6430 N. R. Ortiz
6431 R. M. Cranwell
8024 M. A. Pound
3141 C. M. Ostrander (5)
3151 W. L. Garner (3) for DOE/TIC (Unlimited Release)
DOE/TIC (28)
(C. H. Dalin, 3154-3)

Org.	Bldg.	Name	Rec'd by	Org.	Bldg.	Name	Rec'd by

Sandia National Laboratories